ABSTRACTS

CMDIS

http://cmdis.rpi.edu

FALL SYMPOSIUM 2018

Center for Materials, Devices and Integrated Systems

Rensselaer

INSIDE

WELCOME

Welcome to the second annual CMDIS research symposium. We are delighted to have such a rich and full spectrum of presentations in the is symposium, numbering 61 in total, and spanning the full spectrum of research activities within our center.

The CMDIS enables transformative research that spans the range from fundamental discovery to systems level assembly and manufacturing in the physical / chemical sciences and engineering at Rensselaer. It is responsible for the operation of two major experimental facilities on campus, the microscale and nanoscale fabrication cleanroom (MNCR) and the nanoscale characterization core (NCC). It has around 95 faculty members, 120 student and postdoc members, and five affiliated centers (SCOREC, CFES, CASE, LESA and CATS). Our student and postdoc program was initiated within the last year and is growing rapidly, with activities to date including establishing research focus groups (eight to date) and events such as career evenings and instrument tutorials. For more information see http://cmdis.rpi.edu and please let us know how you would like to participate.

During the day, please be sure to interact with your colleagues, ask them questions about their research, and tell them about your research. We hope that many new connections and collaborations are initiated today, and that you enjoy the event!

Finally, many thanks to Dr. Deniz Rende for her superb work in organizing this symposium.

With best wishes,

Robert Hull,

Associate Vice President, Sr.
Director, Rensselaer Center for Materials, Devices and Integrated Systems

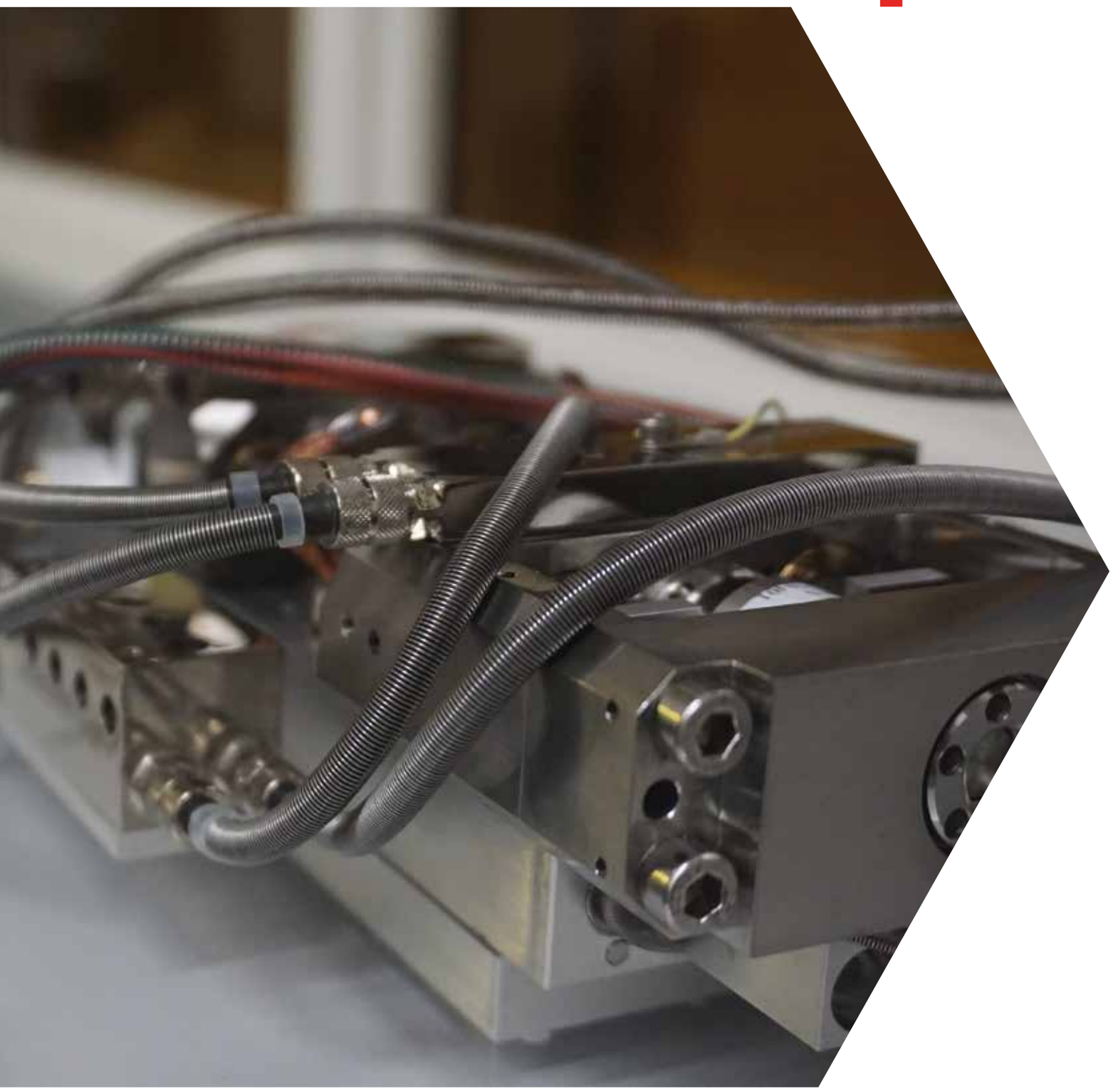

RESEARCH @ THE CENTER

Research at the CMDIS spans the broad spectrum of the physical and chemical sciences and engineering, supporting advances in new materials, devices, and systems.

ADVANCED COMPUTATIONAL DEVICES: New materials, devices and circuit designs for advancing the state-of-the art in computation, including studies of electronic transport at the nanoscale, THz-level circuit design, and materials for cognitive computing.

ADVANCED POLYMERIC MATERIALS: Creation and discovery of new polymeric structures and properties with applications such as 3D-assembly, novel energy systems, and optical / electronic devices.

ENERGY SOLUTIONS: Research spanning new methods for energy storage, generation and transmission, including thermoelectric materials, advanced photovoltaic materials, and optimizing the energy grid.

ELECTROCHEMICAL SYSTEMS: Broad applications to fundamental mechanisms of corrosion, advanced battery systems, and nuclear waste storage.

INTERFACIAL ENGINEERING AND 2D SYSTEMS: Creation of enhanced interfacial property combinations using molecular interlayers and synthesis, processing and characterization of new atomically thin layered systems with novel properties.

MATERIALS INFORMATICS AND DATA ANALYTICS: Developing new methodologies for prediction of new materials with improved properties, and for maximizing extraction of information from data.

MODELING AND SIMULATION: An extensive modeling and simulation eco-system, spanning first principles to atomistic to continuum methods, supported by one of the most powerful supercomputers on a US academic campus.

NANOSTRUCTURED SYSTEMS: Fundamental research into creation of new structures at the nanoscale, with new property combinations, and novel opportunities for system assembly, particularly at the biological-abiotic interface.

PROCESSING AND MANUFACTURING RESEARCH: New methods for materials processing and assembly, spanning a broad range of materials, structures, robotics, control, and advanced manufacturing methods.

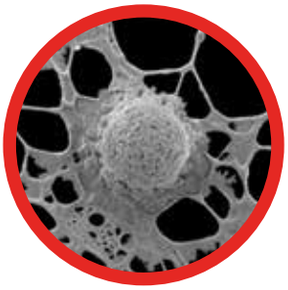

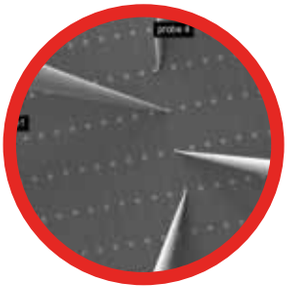

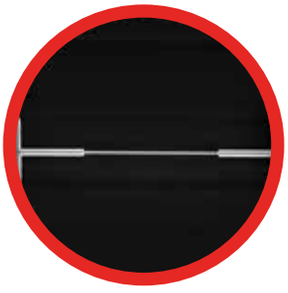

FACILITIES @ THE CENTER

The CMDIS supports two major experimental facilities:

The Microscale and Nanoscale Cleanroom (MNCR) has 5,800 sqft, Class 100 space and contains a broad range of processing, measurement, and fabrication tools enabling researchers to create new structures, devices, and systems at the micro and nano-scale.

ANNEALING
DEPOSITION
ETCHING
SAMPLE PREPARATION
LITHOGRAPHY
METROLOGY

The Nanoscale Characterization Core (NCC) has 3,300 sqft space and provides a powerful suite of imaging, spectrometry, and diffraction instruments to interrogate structure, chemistry, and other properties from the atomic- to micro-scales.

DIFFRACTION
MICROSCOPY
ELECTRICAL TESTING
SPECTROSCOPY
MECHANICAL TESTING
THIN FILMS

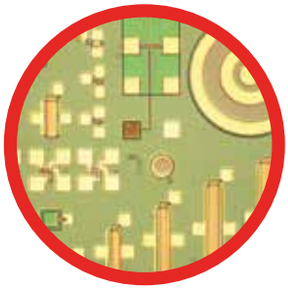

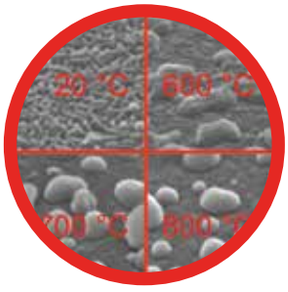

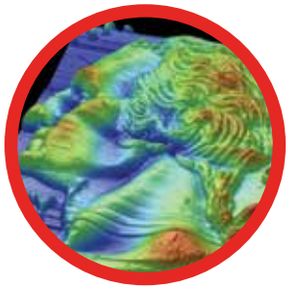

PROGRAM AT-A-GLANCE

8:30 – 9:00	**Registration and breakfast**
9:00 – 9:15	**Welcome** **Robert Hull** *Director, Center for Materials, Devices and Integrated Systems*
9:15 – 10:45	**OP.01 | Debjit Ghoshal** *Catalyst Free Morphology Controlled Growth of 2D perovskite nanowires for polarization detection* **OP.02 | Yu Xiang** *2D Materials in Real and Reciprocal Spaces: Complimentary AFM and RHEED Studies* **OP.03 | Damien Tristant** *Vibrational Analysis Beyond the Harmonic Regime in Few-Layer Black Phosphorus* **OP.04 | Donovan Weiblen** *Influence of Nanoparticle Surface Chemistry on Properties of Iron Oxide–Poly(ethylene oxide) Nanocomposites* **OP.05 | Anthony Yoshimura** *First principles simulation of local response in two-dimensional transition metal dichalcogenides under electron irradiation* **OP.06 | Maria Daniela Barrios Perez** *Computational Investigation of ions and biological peptide translocation through MoS_2 Nanopores*
10:45 – 11:05	**Coffee Break and Networking**
11:05 – 12:05	**OP.07 | Venkata Siva Varun Sarbada** *Crystallization studies of ultra thin Li-V-O thin films* **OP.08 | Siddharth Joshi** *Facile Synthesis of Large Area Two Dimensional Layers of Transition Metal Nitride and Their Use as Insertion Electrodes* **OP.09 | Prateek Hundekar** *In Situ Healing of Dendrites in a Potassium Metal Battery* **OP.10 | Indroneil Roy** *Oxides of Manganese as Efficient Bifunctional Electrocatalysts*
12:05 – 12:45	**Lunch (Great Room)**
12:45 – 1:45	**Poster Session (Great Room)**

Continued >>>

12:45 – 1:45	**Poster Session (Great Room)**
1:45 – 3:00	**OP.11 | Andrew Cupo** *Theoretical Analysis of Spectral Lineshapes from Molecular Dynamics* **OP.12 | Arun Baskaran** *Phase field method coupled with microelasticity theory to model microstructure evolution in Ti-6Al-4V alloys* **OP.13 | Natalya Sheremetyeva** *Low-frequency Raman signature of Ag-intercalated MoS_2: a first-principles study* **OP.14 | Amrita Sarkar** *Block Copolymer Self-Assembly Control on Advanced Nanostructured Materials Fabrications* **OP.15 | Mirco Sorci** *Membrane filtration: Understanding particle intrusion through fundamental measurements and simulations*
3:00 – 3:15	**Coffee Break and Networking**
3:15 – 4:30	**OP.16 | Erik Milosevic** *Metals for High-Conductivity Narrow (10 nm) Interconnects* **OP.17 | Sagnik Nath** *Scalable Integration of Single Flux Quantum (SFQ) Circuits into VLSI Design Flow using commercial EDA tools* **OP.18 | Fabio Filipe Ferreira Garrudo** *Conductive Polyaniline-PCL electrospun fibers for neuron regeneration* **OP.19 | Xiang Zhou** *Performance Limits of Vertical 4H-SiC and 2H-GaN Superjunction Devices* **OP.20 | Pranesh Navarathna** *Towards Automated Logging and Activity Prediction for People with Diabetes using Smart Devices*
4:30 – 6:00	**Concluding Remarks and Awards** **CMDIS Holiday Reception (Great Room)**

AiS.01

GENEVIEVE KANE
TAKE A WALK THROUGH MY POST APOCALYPTIC GARDEN

AiS.02

DONOVAN WEIBLEN
A STRANGE NEW WORLD

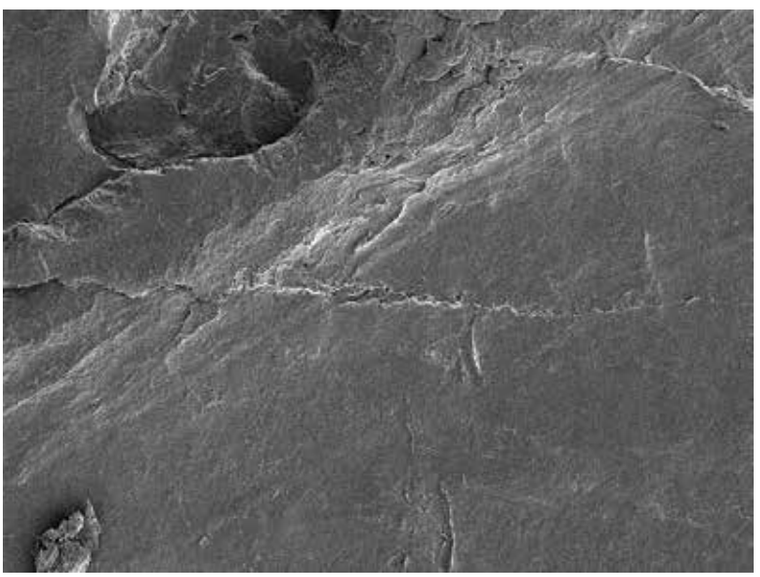

AiS.03

VENKATA SIVA VARUN SARBADA
RAINY DAY IN THE CITY

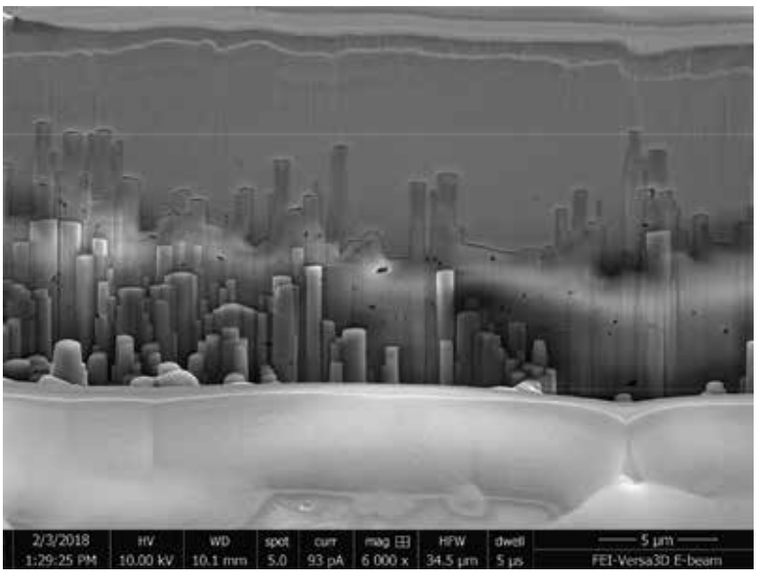

AiS.04

FABIO FILIPE FERREIRA GARRUDO
HORSE SADDLE

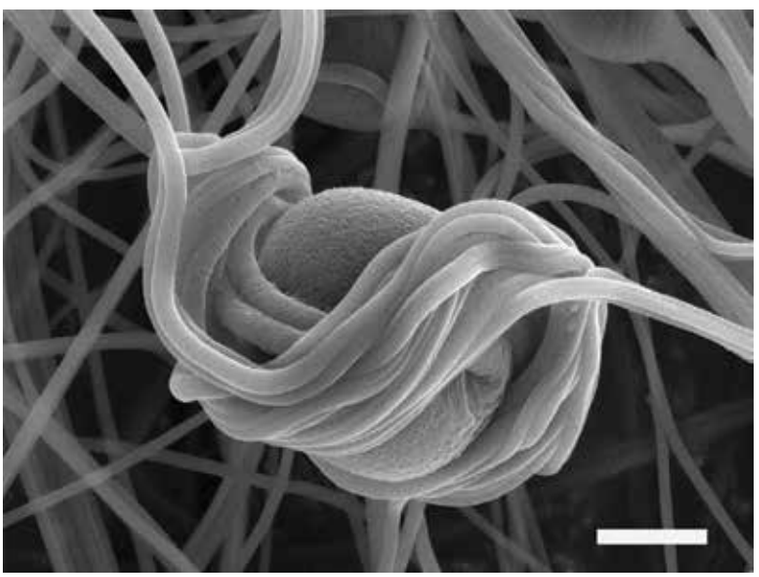

Horse Saddle: when researching new materials, always keep in mind the possible applications. Polybenzimidazole 13% fibers (electroconductive polymer) was electrospun. Fiber mat was coated with gold-paladium and imaged with VERSA-SEM, 5kV. Average diameter = 131±37nm (30.000x magnification).

AiS.05

PRATEEK HUNDEKAR
DONKEY WITH HIS TONGUE OUT

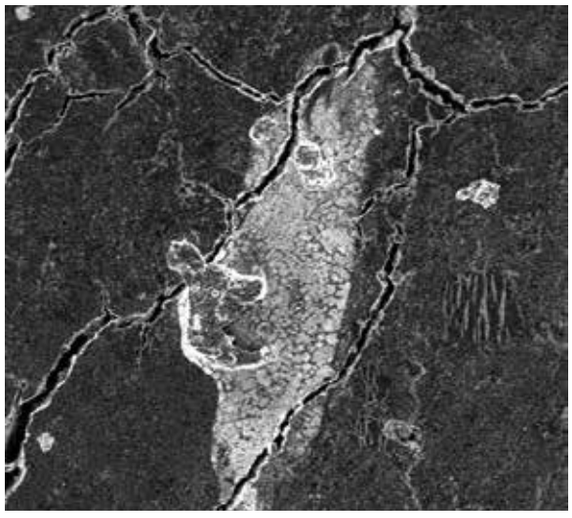

AiS.06

MIRCO SORCI
LIVE FIBROBLAST CELL IMAGED IN CULTURE MEDIUM USING AFM

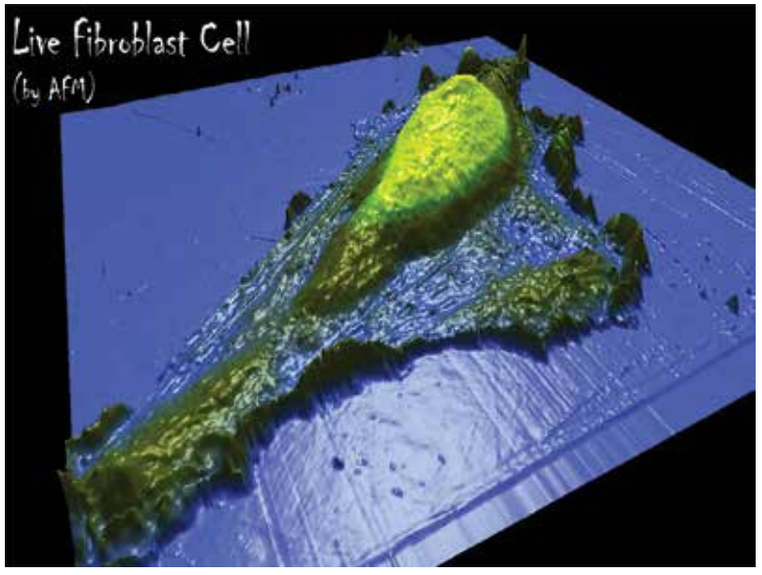

AiS.07

INDRONEIL ROY
BLOOMING METAL OXIDE PLATELETS

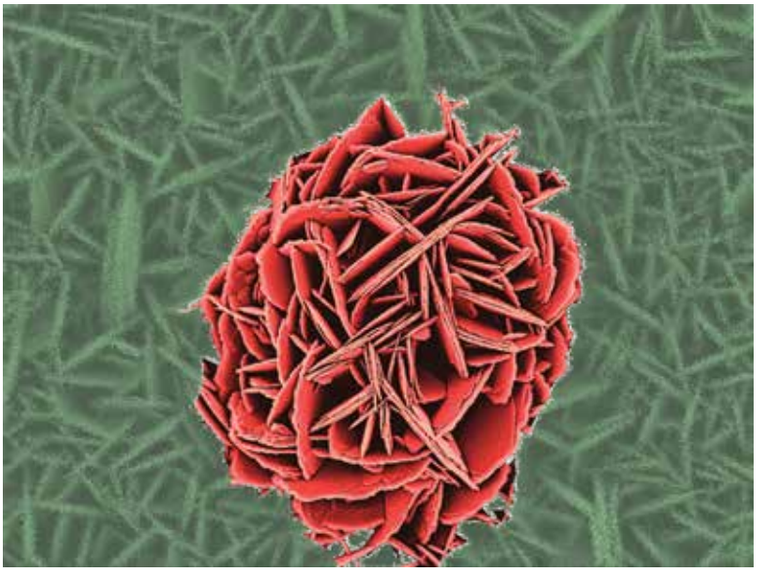

Acknowledgement:
Siddharth Joshi (joshis3@rpi.edu)
Nick Smieszek (smiesn2@rpi.edu)

AiS.08

GENEVIEVE KANE
LOST IN THE DARKNESS - THE FOREST OF GRAD SCHOOL

AiS.09

GWO-CHING WANG
BALANCING ACT DEFIES GRAVITY

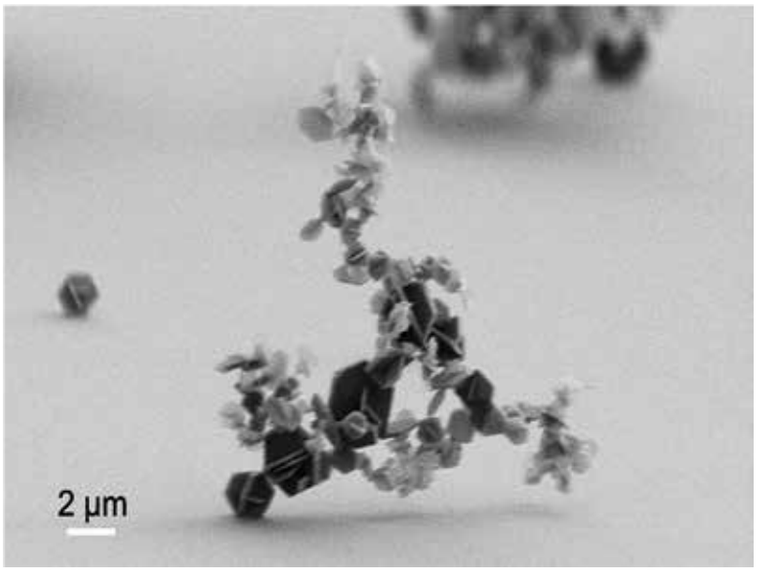

AiS.10

AMRITA SARKAR
A TURBULENT NANOOCEAN

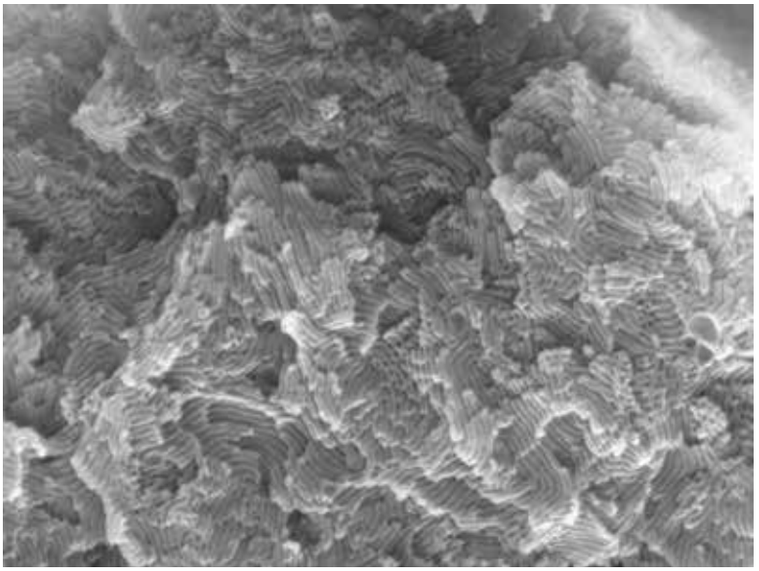

AiS.11

SIDDHARTH JOSHI
MXENE CHRISTMAS MORNING

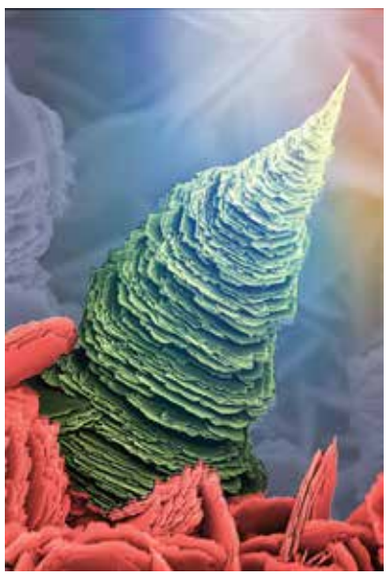

Acknowledgement:
Indroneil Roy (royi@rpi.edu)

OP.01 DEBJIT GHOSHAL
9:15 – 9:30

Catalyst Free Morphology Controlled Growth of 2D perovskite nanowires for polarization detection

Debjit Ghoshal[1,2], Tianmeng Wang[1,2], Nikhil Koratkar[3,4] and Su-fei Shi[1,5]

1 Department of Chemical and Biological Engineering, Rensselaer Polytechnic Institute, Troy, NY, 12180, United States
2 Center for Materials, Devices and Integrated Systems, Rensselaer Polytechnic Institute, Troy, NY, 12180, United States
3 Department of Mechanical, Aerospace and Nuclear Engineering, Rensselaer Polytechnic Institute, Troy, NY, 12180, United States
4 Department of Material Science and Engineering, Rensselaer Polytechnic Institute, Troy, NY, 12180, United States
5 Department of Electrical, Computer, and Systems Engineering, Rensselaer Polytechnic Institute, Troy, NY, 12180, United States

contact: ghoshd2@rpi.edu

2D perovskites have emerged as a class of material inheriting the advantages of two different classes of materials with superior optoelectronic properties, perovskites and 2D materials. The large exciton binding energies and natural quantum well structure can hence not only serve as ideal platforms to study strong light matter interaction but also can be used for various functional optoelectronic devices. Nanoscale structuring and morphology control of semiconducting materials has led to semiconducting materials with enhanced functionalities. Nanowires of semiconducting materials have been extensively used for important applications like lasing and sensing. Catalyst assisted VLS techniques and template assisted growth have conventionally been used for nanowire growth but have several limitations. However, catalyst and template free scalable growth with morphology control of these 2D perovskites has remained elusive. In this manuscript, we demonstrate a facile approach for morphology controlled growth of high quality nanowires of 2D perovskite $(BA)_2PbI_4$. We show the photoluminescence from the nanowires are highly polarized with a polarization ratio as large as 0.73. Finally, we demonstrate that the photocurrent from nanowire/graphene heterostructure is also highly polarization dependent with the photocurrent anisotropy ratio of 3.62, thus demonstrating the use of these nanowires as highly efficient polarization photodetectors.

OP.02 YU XIANG
9:30 – 9:45

2D Materials in Real and Reciprocal Spaces: Complimentary AFM and RHEED Studies

Y. Xiang[1], X. Sun[1], Z. Lu[1], X. Zhang[2], M. A. Washington[1], J. M. Redwing[2], T.-M. Lu[1] and G.-C. Wang[1]

1Department of Physics, Applied Physics and Astronomy, Rensselaer Polytechnic Institute, Troy, 12180

2 Department of Materials Science and Engineering, The Pennsylvania State University, University Park, 16802

contact: xiangy@rpi.edu

There has been an explosive growth in the study of 2D materials due to their novel electronic, electrical, optical, and magnetic properties. The structure of a 2D material not only strongly affects the properties of the material itself but also influences the epitaxial growth of other 2D materials when it is used as a template. However, a layer or a few-layers thick material is challenging to characterize due to the fact that the total number of atoms in the layer(s) is small compared with that of a thick layer. The current push for a quantitative characterization of the symmetry and perfection of those 2D materials deposited on or transferred to a surface has triggered us to apply surface sensitive techniques such as Reflection High Energy Electron Diffraction (RHEED) and Atomic Force Microscopy (AFM) in 2D systems.

While RHEED tells us the crystal structural information in reciprocal space, AFM gives real space morphological information. They are complimentary to each other. In this report, we present the RHEED and AFM studies of two common 2D materials: a single crystal monolayer graphene on an amorphous SiO_2 substrate sample and a monolayer WSe_2 on the c-plane sapphire sample. We demonstrate the use of RHEED to map out the reciprocal space structure (Fig. 1a) and the use of AFM to measure the layer thickness and surface roughness of those materials (Fig. 1b). We show that both techniques can be used to determine the interlayer spacing of the 2D material and they agree with each other within experimental uncertainty.

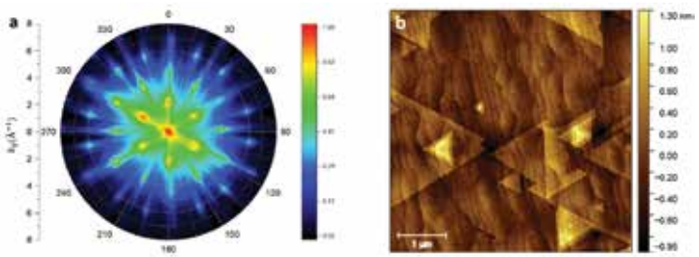

Figure 1. (a) RHEED reciprocal space mapping and (b) AFM image from the WSe_2 on sapphire sample

Acknowledgements: This work is supported by NSF DMR-1539916, and NY State Empire State Development's Division of Science, Technology and Innovation (NYSTAR) through Focus Center Contract C150117 and Rensselaer.

OP.03 DAMIEN TRISTANT

9:45 – 10:00

Vibrational Analysis Beyond the Harmonic Regime in Few-Layer Black Phosphorus

Damien Tristant[1], Andrew Cupo[1], Xi Ling[2], and Vincent Meunier[1]

1 Department of Physics, Applied Physics, and Astronomy, Rensselaer Polytechnic Institute, Troy, NY 12180
2 Division of Materials Science and Engineering, Boston University, Boston, MA 02215

contact: tristd@rpi.edu

In non-metallic materials the heat transfer is dominated by phonons, the quanta of vibrational modes. At 0 K, the vibrational properties of nanostructures can be studied based on the harmonic model. However, harmonic phonons are non-interacting, have an infinite lifetime and the corresponding thermal conductivity is infinite. Therefore, a more realistic approach needs to include the phonon anharmonicity, which results in phonon-phonon scattering.

Black phosphorus (BP) features a tunable band gap and its high electrical conductivity and low thermal conductivity along the armchair direction make it a promising material for thermoelectric devices. In this work, we report a Raman spectroscopy study of few-layer BP with varied incident polarization. The active modes A_g^1, B_{2g} and Ag^2 exhibit a frequency downshift, while the linewidth tends to increase with increasing temperature. To understand the details of these phenomena, we perform first-principles density functional theory calculations on freestanding single-layer BP. The effect of thermal expansion is included by imposing the temperature dependent lattice constant. The temperature induced shift of the phonon frequencies is carried out using ab initio molecular dynamics simulations. The normal mode frequencies are calculated by identifying peak positions from the magnitude of the Fourier transform of the total velocity autocorrelation. Anharmonicity induces a frequency shift for each individual mode and the three- and four-phonon process coefficients are extracted. These results are also obtained from many-body perturbation theory, giving access to phonon lifetimes and lattice thermal conductivity. In general, these theoretical results are in good agreement with experiment.

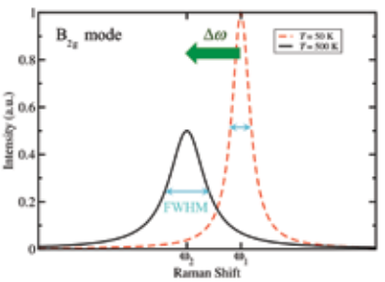

OP.04 DONOVAN WEIBLEN

10:00 – 10:15

Influence of Nanoparticle Surface Chemistry on Properties of Iron Oxide– Poly(ethylene oxide) Nanocomposites

Donovan Weiblen[1], Grace Gionta[2], Deniz Rende[3], Pinar Akcora[4], Rahmi Ozisik[1,3]

1 Department of Materials Science and Engineering, Rensselaer Polytechnic Institute, Troy, NY 12180,
2 Department of Chemical and Biological Engineering, Rensselaer Polytechnic Institute, Troy, NY 12180,
3 Center for Materials, Devices, and Integrated Systems, Rensselaer Polytechnic Institute, Troy, NY 12180,
4 Department of Chemical Engineering and Materials Science, Stevens Institute of Technology, Hoboken, NJ 07030

contact: weibld@rpi.edu

Heating using magnetically susceptible nanoparticles has shown promise in biomedical applications in areas such as tissue engineering and drug delivery. In the current work, the effect of surface coating on iron oxide nanoparticles heated via an alternating magnetic field (AMF) was explored. Two coatings were investigated in addition to bare nanoparticles: poly(ethylene glycol), PEG, coated and amine coated 50–nm–diameter iron oxide nanoparticles. These nanoparticles were dispersed in concentrations varying from 0.010–0.750% by weight in poly (ethylene oxide), PEO. PEO was chosen due to its known biocompatibility and use in the healthcare industry. A significant increase in temperature was observed considering the low loading of particles in all samples. Analysis of heating curves revealed an unusual result. The amine coated particles had a much more significant and rapid response than either the uncoated or PEG coated nanoparticles. Healing properties of samples were also investigated as a function of AMF parameters and iron oxide surface chemistry.

Acknowledgements: This material is based upon work supported by the National Science Foundation under Grant No. CMMI-1825254. The authors would also like to acknowledge use of the Nanoscale Characterization Core within the Center for Materials, Devices, and Integrated Systems at RPI.

OP.05 ANTHONY YOSHIMURA

10:15 – 10:30

First principles simulation of local response in two-dimensional transition metal dichalcogenides under electron irradiation

Anthony Yoshimura[1] and Vincent Meunier[1,2]

1 Department of Physics, Applied Physics, and Astronomy, Rensselaer Polytechnic Institute, Troy, New York 12180, USA

2 Department of Materials Science and Engineering, Rensselaer Polytechnic Institute, Troy, NY 12180, USA

contact: yoshia@rpi.edu

Electron beam irradiation by transmission electron microscopy (TEM) is a common and effective method for post-synthesis defect engineering in two-dimensional transition metal dichalcogenides (TMDs). Combining density functional theory (DFT) with relativistic scattering theory, we simulate the generation of such defects in monolayer group-VI TMDs, MoS_2, WS_2, $MoSe_2$, and WSe_2, focusing on two fundamental TEM- induced atomic displacement processes: chalcogen sputtering and vacancy migration. Our calculations show that the activation energies of chalco- gen sputtering depend primarily on the chalcogen species, and are smaller for TMDs containing Se. Meanwhile, vacancy migration activation ener- gies hinge on the transition metal species, being smaller in TMDs containing Mo. Incorporating these energies into a relativistic, temperature- dependent cross section, we predict that, with appropriate TEM energies and temperatures, one can induce migrations in all four group-VI TMDs without simultaneously producing vacancies at a significant rate. This can allow for controlled manipulation of the TMD crystal for targeted functionality, without the risk of substantial collateral damage.

OP.06 MARIA DANIELA BARRIOS PEREZ

10:30 – 10:45

Computational Investigation of Ions and Biological Peptide Translocation Through MoS_2 Nanopores

Maria Daniela Barrios[1], Adrien Nicolaï[1], Patrice Delarue[1], Vincent Meunier[2], Marija Drndic[3], Patrick Senet[2]

1 Laboratoire Interdisciplinaire Carnot de Bourgogne, UMR 6303 CNRS-Université de Bourgogne Franche-Comté, 9 Av. A. Savary, BP 47 870, F-21078 Dijon Cedex, France,

2 Department of Physics, Applied Physics, and Astronomy, Rensselaer Polytechnic Institute,110 8th street, Troy, NY 12180, USA,

3 Department of Physics and Astronomy, University of Pennsylvania, Philadelphia, Pennsylvania, 19104, USA

contact: maria-daniela.barrios-perez@u-bourgogne.fr

Solid-state nanopores (SSN) made of two-dimensional materials such as molybdenum disulfide (MoS_2), have emerged as versatile tools for biomolecule detection. One of the most promising features of SSN is the sequencing of DNA and protein, at a low cost and faster that the current standard methods, with potential applications for disease diagnosis. SSN sequencing experiments are based on the measurement of ionic current variations when a biomolecule in ionic solution isdriven through a nanopore by applying an externalvoltage. As the biomoleculetranslocates through the nanopore, it occupies the pore volume, blocking the passage of ions. Therefore, ultrafast monitoring of ionic flow during the passage of the biomolecule yields information about its structure and chemical properties. In this work, we investigate the feasibility of using MoS_2 nanopores for protein sequencing from all-atom molecular dynamics (MD) simulations. First, we study the ionic conductivity of KCl electrolyte through sub 5-nmnanopores and we provide an improved model thatwould be useful for experimentalists to interpret their conductance data. Second, we study the translocation of Lysine residues and the use of poly-Lysine tag attached to biological peptides as a potential method to control the translocation of proteins through SSN. Finally, we report the relationship existing between the translocation events observed and the ionic conductance signal computed during MD trajectories.

Acknowledgements: The simulations were performed using HPC resources from DSI-CCuB (Université de Bourgogne). The work was supported by a grant from the Air Force Office of Scientific Re- search (AFOSR), as part of a joint program with the Directorate for Engineering of the National Science Foundation (NSF), Emerging Frontiers and Multidisciplinary Office grant No. FA9550-17-1-0047 and by the NSF Grant EFRI 2-DARE (EFRI- 1542707). The authors also thank the Conseil Régional de Bourgogne-Franche Comté for the funding (grant ANER NANOSEQ).

OP.07 VENKATA SIVA VARUN SARBADA

11:05 – 11:20

Crystallization studies of Ultra-thin film Li-V-O Cathodes

Varun Sarbada[1] , Andrew K. Kercher[2] , Qing Zhang[3] , Danielle J. Cherniak[4], Amy C. Marschilok[3,5,6], Esther S. Takeuchi[3,5,6], Kenneth J. Takeuchi[3,5], Nancy J. Dudney[2] and Robert Hull[1,7]

1 Department of Materials Science and Engineering, Rensselaer Polytechnic Institute, Troy, NY 12180
2 Materials Science & Technology Division, Oak Ridge National Laboratory, Oak Ridge, TN 37830
3 Department of Materials Science and Chemical Engineering, Stony Brook University, Stony Brook, NY 11794
4 Department of Earth and Environmental Sciences, Rensselaer Polytechnic Institute, Troy, NY 12180
5 Department of Chemistry, Stony Brook University, Stony Brook, NY 11794
6 Energy Sciences Directorate, Brookhaven National Laboratory, Upton, NY 11973
7 Center for Materials, Devices and Integrated Systems, Rensselaer Polytechnic Institute, Troy, NY 12180

contact: sarbav@rpi.edu

Thermal annealing experiments both in the vacuum of a transmission electron microscope (TEM) and in an Ar environment were performed to understand the crystallization of amorphous Li-V-O thin films (50-100 nm) sputter deposited from a LiV_3O_8 target, as part of a broader study to optimize LiV_3O_8 thin film electrodes for battery application.It is observed that the annealing atmosphere (vacuum vs Ar) has a profound effect on the Li-V-O phase crystallized. Depending on annealing atmosphere and temperature, delithiated phases such as V_2O_5, V_2O_3 and VO_2 were generated, but not the desired LiV_3O_8 stoichiometry. Compositional depth analysis using nuclear reaction analysis (NRA) suggests that lithium diffusion from the Li-V-O film into the substrate and/or lithium loss from the thin film surface can limit the ability to maintain the Li concentration required for forming desired/expected Li-V-O phases (in this case LiV_3O_8) suitable for battery applications. X-ray diffraction, NRA, focused ion beam (FIB) and TEM analysis showed that thicker Li-V-O films (~1 µm) did form the LiV_3O_8 phase within the interior of the film upon annealing in an Ar environment, but formed the Li-deficient $Li_{0.3}V_2O_5$ phase at the film surface. In this work, combined nano- and micro-scale diffraction, spectroscopic and imaging analysis provide the necessary understanding regarding the Li concentration depth profile and phase distributions in such films, for future development of thin film battery systems.

Acknowledgements: This work was supported as part of the Center for Mesoscale Transport Properties, an Energy Frontier Research Center supported by the U.S. Department of Energy, Office of Science, Basic Energy Sciences, under award #DE-SC0012673. Work at RPI made extensive use of the facilities in the Center for Materials, Devices and Integrated Systems (cMDIS). We gratefully acknowledge provision of facilities for NRA measurements at the Ion Beam Laboratory at SUNY Albany.

OP.08 SIDDHARTH JOSHI

11:20 – 11:35

Facile Synthesis of Large Area Two Dimensional Layers of Transition Metal Nitride and Their Use as Insertion Electrodes

Siddharth Joshi,[1] Qi Wang,[1] Ajinkya Puntambekar,[1] and Vidhya Chakrapani[1,2]

1 Howard P. Isermann Department of Chemical and Biological Engineering, Rensselaer Polytechnic Institute, Troy, NY-12180

2 Department of Physics, Applied Physics, and Astronomy, Rensselaer Polytechnic Institute, Troy, NY-12180

contact: chakrv@rpi.edu

In recent years, two-dimensional layers of transition metal carbides, nitrides and carbonitrides, also referred to as "MXenes" have been studied for use in a variety of applications such as batteries, supercapacitors and thermoelectric devices. Transition metal nitrides are especially promising as they show a variety of interesting properties such as high conductivity, compositional and surface termination-dependent band gap, high catalytic activity, high melting point and exceptional hardness. They are also ideal for use as lithium ion battery anodes due to their high specific capacity and lower redox potential for Li^+ insertion than their corresponding oxides. We report a new technique for synthesizing large area, vertically oriented two- dimensional (2D) layers of molybdenum nitride (MoN) involving synthesis of 2D nanosheets of MoO_3 using hot-filament chemical vapor deposition and their subsequent nitridation to δ-MoN using ammonia. This two-step process of phase transforming 2D oxide layers potentially enables easy synthesis of a wide variety of MXenes of nitrides, sulfides, and carbides of tunable composition. Using X-ray diffraction, X-ray photoemission spectroscopy and differential capacitance measurements, we show that 2D layers of MoN operate as insertion electrodes as opposed to bulk MoN which operate as conversion electrodes. Unlike conversion electrodes, the crystal lattice in insertion electrodes does not undergo compositional changes and therefore undergo small extent of volumetric expansion. Hence, these electrodes tend to show stable capacity even after several hundred charge-discharge cycles. Our electrodes show a stable capacity of 320 mAh/g after 200 cycles and do not show any loss in their crystallinity.

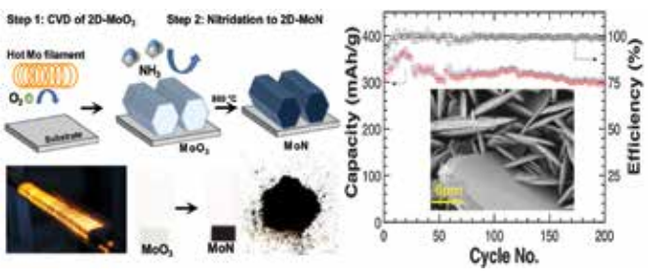

OP.09 PRATEEK HUNDEKAR
11:35 – 11:50

In Situ Healing of Dendrites in a Potassium Metal Battery

Prateek Hundekar[1], Swastik Basu[1], Xiulin Fan[2], Anthony Yoshimura[3], Tushar Gupta[1], Varun Sarbada[3], Lu Li[1], Aniruddha Lakhnot[1], Rishabh Jain[1], Yunfeng Shi[3], Shankar Narayanan[1], Chunsheng Wang[2] and Nikhil Koratkar[1,4]

1 Department of Mechanical, Aerospace and Nuclear Engineering, Rensselaer Polytechnic Institute, Troy, NY, 12180, USA
2 Department of Chemical and Biomolecular Engineering, University of Maryland, College Park, MD, USA
3 Department of Physics, Applied Physics and Astronomy, Rensselaer Polytechnic Institute, Troy, NY, 12180, USA
4 Department of Material Science and Engineering, Rensselaer Polytechnic Institute, Troy, NY, 12180, USA

contact: koratn@rpi.edu

At present, lithium ion batteries (LIBs) dominate the rechargeable battery market. However, potassium ion batteries (KIBs) are emerging as an earth abundant and cheaper alternative to LIBs. The main drawback of KIBs is their lower energy density relative to LIBs, which arises from the increased mass and volume of Potassium (K) compared to Lithium (Li). This drawback could be mitigated by the use of a K-metal anode, which would allow for a much higher specific capacity than carbonaceous, alloying or intercalation compounds, since the packing density of K atoms is the highest in its metallic form. However, as in the case of Li, the K-metal anode is observed to develop dendritic projections during the electrochemical plating- stripping process. The growth of dendrites is associated with a number of problems including irreversible capacity loss, reduced columbic efficiency, drying and degradation of the electrolyte as well as electrical shorting and thermal runaway of the battery. Here, we show that K dendrites can be healed in situ in a K-metal battery. The healing is triggered by current controlled, Joule-heating of the dendrites, which causes migration of surface atoms away from the dendrite tips, thereby smoothening the dendritic surface. While similar effects have been reported in Li-metal batteries, this process is strikingly more efficient in a K-metal battery. We show that the reason for this is the greater "mobility" of surface atoms in K relative to Li metal, which enables the dendrite healing to take place at an order of magnitude lower current density. This *in situ* healing eliminates the risk of short circuiting in KIBs, and thus can be employed as a reliable strategy for the safe deployment of K-metal secondary batteries in high-power applications.

OP.10 INDRONEIL ROY
11:50 – 12:05

Oxides of Manganese as Efficient Bifunctional Electrocatalysts

Indroneil Roy,[1] Qi Wang,[1] and Vidhya Chakrapani,[1,2]

1 Howard P. Isermann Department of Chemical and Biological Engineering, Rensselaer Polytechnic Institute, Troy, NY-12180

2 Department of Physics, Applied Physics, and Astronomy, Rensselaer Polytechnic Institute, Troy, NY-12180

contact: chakrv@rpi.edu

The electrolysis of water, or water splitting reaction is one of the cleanest ways of producing hydrogen and oxygen gas for fuel. Electrochemical devices employing these reactions include regenerative fuel cells and rechargeable metal-air batteries, which have the highest theoretical energy density. Considerable efforts have been dedicated towards improving the energy conversion efficiency of these devices. However, the single main obstacle for achieving this has been the lack of suitable bifunctional oxygen electrocatalysts that show simultaneous high activity for both oxygen reduction (ORR) and oxygen evolution (OER) reactions during charge/discharge cycles. The overpotential and slow kinetics of oxygen reactions are limiting parameters in the advancement of electrochemical storage devices. Taking inspiration from nature's photosynthetic process that uses a Mn_4O_4Ca cluster in photosystem II to catalyze water splitting, we studied the efficiency of various phases of manganese oxide (MnO_x) as electrocatalysts for OER and ORR process, including the role of defects on bifunctionality. Cyclic voltammetry was used to prove that Mn_2O_3 is a bifunctional catalyst by showing high activity for OER and ORR. Next, *in-situ* UV-Vis absorbance spectroscopy was conducted to track changes in the surface oxidation state as a result of occurring reactions. Finally, we use electrochemical quartz crystal microbalance to track ion intercalation into the material. Results from these studies were used to obtain a structure-defect-function correlation that can aid in better design electrocatalysts with bifunctional properties.

Acknowledgements: The authors would like to thank Rensselaer Polytechnic Institute (RPI) and National Science Foundation, CBET award (No: 1511733), for the partial financial support and Nicholas Smieszek for his assistance with the preparation of this manuscript. I.R, and Q.W also gratefully acknowledge the partial support of Howard P. Isermann fellowship provided by the Department of Chemical and Biological Engineering at RPI.

OP.11 ANDREW CUPO
1:45 – 2:00

Theoretical Analysis of Spectral Lineshapes from Molecular Dynamics

Andrew Cupo[1], Damien Tristant[1], Vincent Meunier[1]

1 Department of Physics, Applied Physics, and Astronomy, Rensselaer Polytechnic Institute, Troy, NY 12180

contact: cupoa@rpi.edu

When atoms vibrate about their equilibrium positions in a material, the anharmonicity in the potential energy surface causes coupling between phonons. This in turn renormalizes the harmonic phonon frequencies and produces finite phonon lifetimes. The anharmonicity can be captured non-perturbatively by using molecular dynamics, and temperature dependent phonon properties can be obtained subsequently by analyzing the Fourier transform of the velocity autocorrelation. We develop a theoretical framework that produces exact analytical expressions for the lineshapes of the peaks in these spectra and include the effect of the frequency shift, lifetime, and simulation broadening. The theory is applied to a toy model and graphene, and we demonstrate about at least an order of magnitude reduction in the required simulation time to obtain converged properties as compared to the standard extraction procedure.

Acknowledgements: Part of this work was performed using supercomputing resources provided by the Center for Computational Innovations (CCI) at Rensselaer Polytechnic Institute. AC was supported by NSF Grant EFRI 2-DARE (EFRI-1542707). DT acknowledges support from the Office of Naval Research.

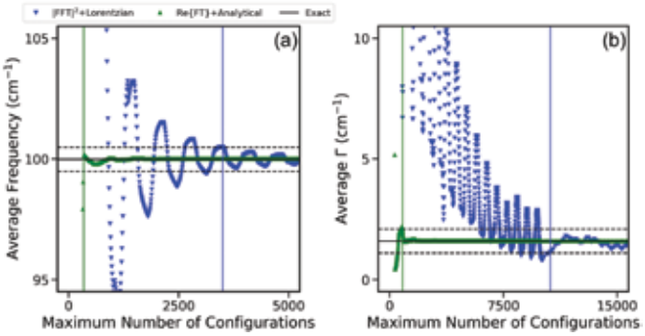

OP.12 ARUN BASKARAN
2:00 – 2:15

Phase field method coupled with microelasticity theory to model microstructure evolution in Ti-6Al-4V alloys

Arun Baskaran[1] , Daniel J Lewis[1]

1 Department of Materials Sci. and Eng, Rensselaer Polytechnic Institute, Troy, 12180

contact: baskaa2@rpi.edu

A multi-phase field model, coupled with microelasticity theory, is implemented to study the microstructural evolution during solid state transformation in Ti-6Al-4V(Ti64). Ti64 is a dual phase alloy, and the coexisting thermodynamic phases are α (HCP) and β (BCC), with the equilibrium β-transus occurring at 995°C. Orientational relationship between α and β and crystal symmetry constraints result in twelve different α-variants that can nucleate from the β matrix. Certain morphological features in Ti64 microstructures,such as basket-weave and colony, area direct result of the presence or absence of preferential variant selection. Since subtle changes in these morphologies influence mechanical properties such as fracture toughness and fatigue, it is important to better understand the influence of processing conditions and alloy history on microstructural evolution. Augmenting a basic phase field model with crystallographic symmetry and orientational relationship between the two phases has enabled us to model the evolution of all twelve unique α-variants. Furthermore, by extending this model to a multi-phase formalism, we are able to simultaneously simulate the growth and evolution of multiple α-variants in three-dimensions. Coupling our model with microelasticity theory will enable us to study how strain energy impacts the influence of processing conditions on α-variant selection. The calculation of elastic strain associated with a solid state phase transformation is adopted from Khachaturyan's paradigm, in which the relaxation strain is divided into homogeneous (shape-affecting) and heterogeneous (maintaining coherency at interfaces) strain components. The phase field model is implemented on a mesh based data structure adopted from MMSP, on the C++ platform. The code is parallelized using the MPI library, and subsequently implemented on BG/Q.

Acknowledgements: This research is sponsored through a grant from the National Science Foundation, Award CMMI-1729336, DMREF: Adaptive control of Microstructure from the Microscale to the Macroscale.

OP.13 NATALYA SHEREMETYEVA

2:15 – 2:30

Low-frequency Raman signature of Ag-intercalated MoS_2: a first-principles study

Natalya Sheremetyeva[1], Drake Niedzielski[1], Damien Tristant[1], Lauren E. Kerstetter[2], Ama Agyapong[2], Anna C. Domask[2], Suzanne Mohney[2] and Vincent Meunier[1]

1 Department of Physics, Rensselaer Polytechnic Institute,110 8thSt, Troy, NY 12180, USA
2 Materials Science and Engineering, Pennsylvania State University, Old Main, State College, PA 16801, USA

contact: sheren@rpi.edu

Two-dimensional layered materials (2DMs) are promising candidates for novel electronic devices due to their tunable electronic properties controlled by the number of layers. For example, bulk MoS_2 has an indirect band gap of 1.29 eV, which becomes a direct band gap of 1.8 eV in a single layer of MoS_2 (Mak K.F. et al., Phys Rev Lett, 105, 136805 (2010)). Precise characterization of 2DMs and their layer number is crucial for exact property control. Raman spectroscopy is a key experimental characterization technique as it is nondestructive and can identify even small structural and electronic changes. With recent advances in Raman spectroscopy hardware it has become possible to resolve low- frequency (LF) Raman response in 2DMs. This response has a relatively lower intensity compared to the high-frequency (HF) Raman signature that is typically studied and is located close to the strong Rayleigh line making the detection challenging. However, the LF Raman peaks belong to LF interlayer modes of 2DMs. These modes correspond to rigid motions of each layer as a whole unit within the 2DM with restoring forces governed by the weak interlayer interactions. These modes are more sensitive to structural parameters such as layer number and stacking order than their HF intralayer counterparts (Liang L. et al., ACS Nano Article ASAP, DOI: 10.1021/acsnano.7b06551). Motivated by experimental results, we present a Density Functional Theory (DFT) based computational study of LF Raman active modes of few-layer MoS_2 intercalated with silver. We predict a noticeable red-shift of the LF modes of MoS_2 upon Ag intercalation and with increasing Ag concentration in few-layer systems. This shift is confirmed experimentally and can be used for confirmation of successful silver diffusion into MoS_2.

Acknowledgements: Supercomputing resources used for this work were provided by the Computational Center for Nanotechnology Innovations (CCNI) at RPI, which is partially supported by the State of New York and IBM.

OP.14 AMRITA SARKAR

2:30 – 2:45

Block Copolymer Self-Assembly Control on Advanced Nanostructured Materials Fabrications

Amrita Sarkar[1], R. Helen Zha[1]

1 Department of Chemical & Biological Engineering, Rensselaer Polytechnic Institute, Troy, NY 12180

contact: sarkaa2@rpi.edu

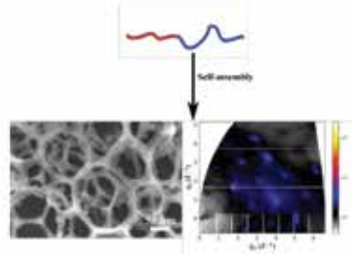

Controlled fabrication of nanostructured materials employing block copolymer self- assembly is in great demand to study the structure-property and performance relationship in high-performance membrane, advanced energy conversion and storage devices. Fundamental study of structure-performance relationship in membrane and energy devices requires tunable nanomaterial where one can tailor pore size and wall-thickness independently. Such an independent control on each architectural feature remains elusive due to reliance upon equilibrium-based approaches where each architectural dimension is subjected to the whims of free energy minimization. On the other hand, well-defined, mechanically strong porous separation membrane derived from block copolymer is challenging to achieve.

To resolve the primary challenge of independent control on architectural feature, a kinetic-controlled approach was introduced, termed as persistent micelle templating (PMT). It is formulated establishing a custom-made block copolymer structure-directing agent, poly(ethyleneoxide-*block*-hexyl acrylate) and a solution processing guideline where the kinetic rates are regulated by adjusting cosolvent amount. It directs to the formation of nanostructured materials with tunable 6-9 nm wall-thickness with ~2Å precision and constant pore diameters of 13 nm with a wide range of inorganic material addition. This approach not only launches a new era to fine-tune small architectural feature limiting micelle chain exchange, it also seamlessly spans from mesopores (~10 nm) to macropores (~200 nm) using very few subset of polymers.

Separately well-defined porous polymer membrane was achieved using a classic block copolymer, poly(styrene-block-lactide) and an acidic etchant. However, the porous polymeric membranes are not showing outstanding mechanical property. Hence, our current work is concentrated towards the development of extra-mechanically strong polymer template. We get inspiration from "Silk" protein which is nature's one of the high-performance supramolecule and shows remarkable mechanical properties via forming β-sheet nanocrystal domain. Recent work is focusing towards the synthesis and nanoscale characterization of advanced "silk" mimetic polymeric material.

OP.15 MIRCO SORCI
2:45 – 3:00

Membrane filtration: Understanding particle intrusion through fundamental measurements and simulations

Mirco Sorci, Corey C. Woodcock, Joel L. Plawsky and Georges Belfort

Howard P. Isermann Department of Chemical and Biological Engineering and the Center of Biotechnology and Interdisciplinary Studies, Rensselaer Polytechnic Institute, Troy, NY 12180- 3590

contact: sorcim@rpi.edu

Many relevant industrial fluids (e.g. cell culture broths, paints, milk, etc.) fall in the category of colloidal suspension (i.e. nanometers to micrometers) and are of great interest in microfiltration. This pressure-driven membrane process, while being one of the oldest, yet remains not fully understood. The major limitation is membrane fouling. Particle deposition onto the microporous membrane, resulting in pore constriction and/or blockage, and eventually in cake formation, has been largely investigated and mitigation strategies have been proposed.

In this study, we are focusing on particles deposition into a microporous membrane, giving particular attention to the role of pore structure and chemistry. The membranes used were 0.2 µm and 5 µm pore size poly(ether sulfone) (PES), since PES is widely used thanks to low unspecific binding and mechanical stability. Silica nanoparticles, 40 nm and 1 µm, respectively, were selected as colloidal suspensions.

***In vitro* studies focused on 2D and 3D characterization of pore distributions, by atomic force microscopy (AFM), scanning electron microscopy (SEM), and focused ion beam SEM (FIB- SEM). In order to understand the forces at place, (i) zeta potential for both membranes was measured using 1-10-100 mM electrolyte solutions in a pH range 4-10; and (ii) AFM in force mode was used to estimate the adhesion force between the membranes and a silica microsphere attached to an AFM probe. Finally filtration experiments were performed using diluted colloidal suspensions (i.e. <1% v/v), and array tomography, combined with SEM imaging, was applied to visualize the distribution of particles into the fouled membranes.**

Taking advantage of the experimental characterization, *in silico* modeling using Comsol Multiphysics software was conducted in parallel to build a better understanding of particle interactions with the membrane walls in the pores. Prototype models will combine pore geometry representation, moving mesh algorithm, flow conditions, forces, to obtain particle tracking trajectories with the goal to narrow down the key features pointing toward optimal membrane performance.

OP.16 ERIK MILOSEVIC
3:15 – 3:30

Metals for High-Conductivity Narrow (10 nm) Interconnects

Erik Milosevic, Sit Kerdsongpanya, Daniel Gall

Department of Materials Science and Engineering, Rensselaer Polytechnic Institute, 110 8th St, Troy, NY 12180

contact: milose@rpi.edu

Epitaxial Ru(0001) and Co(0001) films with thickness d ranging from 5 to 300 nm are sputter deposited onto Al_2O_3(0001) substrates in order to quantify and compare the resistivity size effect. Both metals form single crystal layers with their basal planes parallel to the substrate surface and exhibit a root-mean-square roughness < 0.4 nm for Ru and < 0.9 nm for Co. Transport measurements on these layers have negligible resistance contributions from roughness and grain boundary scattering which allows direct quantification of electron surface scattering. The measured resistivity ρ vs d is well described by the classical Fuchs-Sondheimer model, indicating a mean free path for transport within the basal plane of λ = 6.7 ± 0.3 nm for Ru and λ = 19.5 ± 1.0 nm for Co. Bulk Ru is 36% more resistive than Co; in contrast, Ru(0001) layers with $d \leq 25$ nm are more conductive than Co(0001) layers, which is attributed to the shorter λ for Ru. The determined λ-values are utilized in combination with the Fuchs-Sondheimer and Mayadas- Shatzkes models to predict and compare the resistance of polycrystalline interconnect lines including relevant barrier/adhesion layers. This results in predicted 10 nm half-pitch line resistances for Ru, Co, and Cu of 1.0, 2.2, and 2.1 kΩ/µm, respectively, indicating a 2x conductance advantage of Ru lines in comparison to current-technology Cu lines.

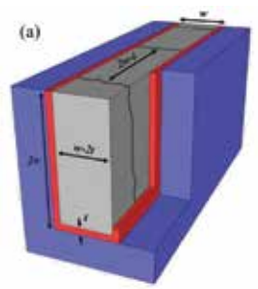

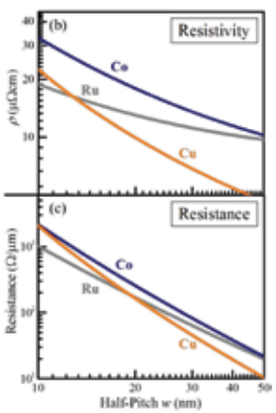

Figure: (a) Schematic of a 2:1 aspect ratio interconnect line with a half-pitch w, a liner thickness t, and a 2w-t grain size along the growth direction. Predicted (b) resistivity and (c)resistance of Ru, Co, and Cu lines vs w.

OP.17 SAGNIK NATH

3:30 – 3:45

Scalable Integration of Superconducting Flux Quantum (SFQ) Circuits into VLSI Design Flow using commercial EDA tools

Sagnik Nath[1] , Kurt English[1] , Alexander Derrickson[1], John F. McDonald [1]

1 Electrical, Computer, and Systems Engineering Department, Rensselaer Polytechnic Institute, Troy, NY-12180

contact: naths3@rpi.edu

Single Flux Quantum (SFQ) circuits, that employ Josephson Junctions as switching elements, offer low power computing alternatives to traditional semiconductor hardware in an era of large scale computing accounting considerably for global power consumption. Improvements in manufacturing techniques and yield for SFQ circuits show the potential of this technology being a prime candidate to deliver low power high frequency microprocessors in the future.

However, SFQ circuit design still lacks a universal scalable VLSI Design flow, a methodology that helped revolutionise MOS circuit design in the 1980s to cope with increasing processor complexity and streamline the various aspects of system design into separate modules. Currently, Process Design Kits (PDK) do exist for SFQ circuit design in commercial Electronic Design Automation (EDA) tools . Yet, there is no underlying design flow that allows the circuit designer to specify any design architecture irrespective of the technology and use the EDA tools to scale it towards implementing the design in a standard cell library of SFQ logic cells.

The present work proposes a scalable SFQ Design methodology that adheres to all the key components of traditional VLSI Design Flow, namely Register Transfer Level (RTL), Synthesis and Place and Route in Layout. At the cell level, dual rail asynchronous cells were developed that behaved like normal CMOS gates in contrast to typical SFQ cells that are synchronous. Scripts were written that could convert any single rail netlist (synthesised from an Hardware Description Language design in RTL phase using EDA tool Design Vision) containing single rail cells into dual rail asynchronous cells. Finally, Auto Placement and Routing using EDA tool Innovus was achieved through specific cell layout design choices that allowed the finished circuit design layout to pass checks by Layout Vs Schematic (LVS) and Design Rule Check (DRC). Thus, using the proposed methodology, any functional design written in an HDL language can be directly converted into a placed and routed SFQ layout circuit without manual design intervention.

OP.18 FABIO FILIPE FERREIRA GARRUDO

3:45 – 4:00

Conductive Polyaniline-PCL electrospun fibers for neuron regeneration

Fábio Garrudo[1,2]; Caitlyn Chapman[1]; Pauline Hoffman[1]; João Silva[1,2]; Ranodhi Udangawa[1], Paiyz Mikael[1]; Carlos Rodrigues[1]; Jorge Morgado[2], Frederico Ferreira[2]; Robert Linhardt[1]

1 Center for Biotechnology & Interdisciplinary Studies, Department of Chemistry & Chemical Biology, Rensselaer Polytechnic Institute, Biotechnology Center 4005, Troy, NY, 12180, USA.
2 Institute for Bioengineering and Biosciences, Instituto Superior Técnico, Universidade de Lisboa, Lisboa, Portugal

contact: fabiogarrudo@gmail.com

Introduction: The use of conductive polymers for neural cells scaffolds, able to sustain cell growth and differentiation, is paramount for the cure of neurodegenerative diseases using cell therapy approaches. Besides having the advantage of enabling direct stimulation of the cells with electricity, mimicking the natural brain environment, their properties can be tailored and lead to a better differentiation of stem cells into neurons. The present research project aimed at developing a biocompactible polyaniline (PANi)-polycaprolactone (PCL) electrospun mat for neuron regeneration. Due to its unique properties, it can ultimately be used for various medical applications.

Materials and Methods: Commercially available PANi, doped with Camphorsulfonic acid, was dissolved with PCL (different proportions) in TFE and/or HFP. The obtained solutions were electrospun (15kV, 15cm, 1mL/h) and the obtained fiber mats were characterized using SEM, ATR-FTIR and TGA. Electroconductivity, mechanical properties and biocompactibility using neural stem cells were also assessed.

Results and Discussion: Obtained fiber diameters are within the nanometer range. FTIR allowed to identify unique peaks that could be correlated with the amounts of PANI for each fiber. TGA's residue amount was correlated with PANI content. FTIR and TGA together indicate that both polymers are blended in the fibers, but not interacting very strongly with each other. Electroconductivity was correlated with PANi/PCL proportion used for the fibers, peaking 1.03E-1 S/cm, higher than most biologic fluids (1.00E-2 S/cm). All fiber matts tested allowed normal cell growth rates. Higher proportion of PANi/PCL was associated with smaller number of cells at day 1. Normal cell morphology, evaluated through SEM and LIVE/DEAD, was kept.

Conclusions: The obtained PANi/PCL fibers can support ReN-VM growth and are conductive enough for electrical stimulation assays. Future studies include studying the differentiation profile of ReN-VM/iPSC cells with electric stimulation and encapsulation of neurotrophic factors for differentiation enhancement.

Acknowledgements: The authors thank the support of the following CBIS cores for all the analysis made: Analytical Biochemistry (Joel Morgan, PhD), Microscopy Research (Sergey Pryshchep, PhD) and CMDIS Nanoscale characterization (Deniz Rende, PhD). The authors also thank the assistance from all the personal from MNCR-cMDIS-RPI cleanroom facility for SEM (Mr David Frey, BSc) and 4-proble analysis (Bryant Colwill, BSc; Sarah An, PhD; John Barthel, BSc) The authors gratefully acknowledge the financial support from FCT through the scholarship PD / BD / 114045 / 2015.

OP.19 XIANG ZHOU
4:00 – 4:15

Performance Limits of Vertical 4H-SiC and 2H-GaN Superjunction Devices

Xiang Zhou[1], T. Paul Chow [1]

Electrical, Computer, and Systems Engineering Department, Rensselaer Polytechnic Institute, Troy, NY-12180

contact: zhoux4@rpi.edu

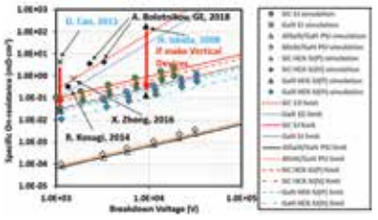

Figure 1. Simulated and calculated Ron,sp versus BV tradeoff curves for 4H-SiC, 2H-GaN vertical p/n superjunction devices, and AlGaN/GaN, AlInN/GaN natural polarization superjunction devices together with reported experimental results

We have determined and evaluated the $R_{on,sp}$ versus BV tradeoff limits of vertical superjunction (SJ) devices for 4H-SiC and 2H-GaN with a previously published analytical model and a new analytical model we developed [1, 2]. For GaN, we have obtained much better performance tradeoffs on the vertical natural polarization superjunction devices based on the AlGaN/GaN or AlInN/GaN heterostructures instead of the conventional pn junctions with alternating p/n pillars. For 1 and 10kV devices, the specific on-resistance is about 1500x and 50000x for natural polarization superjunction devices compared with unipolar 1D limit.

The superjunction (SJ) power devices offer to improve the trade-off between specific on-resistance ($R_{on,sp}$) and breakdown voltage (BV) significantly over conventional devices. The potential performance of SiC and GaN superjunction devices has been projected [3-7]. In addition, in the AlGaN system, natural polarization superjunction, established by inherent spontaneous and piezoelectric polarization across AlGaN/GaN heterojunction, has been demonstrated [8, 9].

The on-resistance of SJ devices will not continue to improve if we keep shrinking the pillar width because of the conducting region consumed by depletion region. We have applied a JFET model to calculate the optimum pitch size by assuming the optimum doping dosage of 1e13cm^{-2} and 2e13cm^{-2} for 4H-SiC and 2H-GaN under charge balance condition. The Ron,sp versus the pillar width are plotted for 4H-SiC and 2H-GaN stripe-cell (STR) and hexagonal-cell (HEX) superjunction devices at different drain voltages with simulation results. Furthermore, by assuming a rectangular electric field profile in SJ devices, we get the Ron,sp versus BV trade-off limits for vertical 4H-SiC and 2H-GaN superjunction devices. In addition, employing natural polarization superjunctions using strained $Al_{0.6}Ga_{0.4}N$/GaN or unstrained $Al_{0.82}In_{0.18}N$/GaN (10nm/20nm) heterostructures, we have further substantially reduced the specific on-resistance of vertical SJ devices, reaching 0.06 to 3 μΩ·cm^2 level for the BV range of 1kV to 50kV.

References: **[1]** D. Disney et al., Proc. Int. Symp. Power Semicond. Dev. and IC's, pp. 157-160, 2008. **[2]** H. Kang et al., IEEE Trans. Electron Devices, vol. 65, p. 1432, 2018. **[3]** L. Zhu et al., Int. J. High Speed Electr Syst, vol. 14, p. 865, 2004. **[4]** Z. Li et al., IEEE Transactions on Electron Devices, vol. 60, no. 10, pp. 3230-3237, 2013. **[5]** R. Kosugi et al., Proc. Int. Symp. Power Semicond. Dev. and IC's, pp. 346-349, 2014.**[6]** X. Zhong et al., Proc. Int. Symp. Power Semicond. Dev. and IC's, pp. 231-234, 2016. **[7]** A. Bolotnikov et al., 12th European Conf. Silicon Carbide and Related Materials - ECSCRM 2018. **[8]** H. Ishida et al., IEEE Electron Device Letters, vol. 29, no. 10, pp. 1087-1089, 2008. **[9]** D. S. Cao et al., Chinese Phys. Lett., vol. 28, no. 1, p. 017303, 2011. **[10]** X. Zhou et al., Mater. Sci. Forum, to be published. **[11]** X. Zhou et al., Electron Device Lett., to be published.

OP.20 PRANESH NAVARATHNA
4:15 – 4:30

Towards Automated Logging and Activity Prediction for People with Diabetes using Smart Devices

Pranesh Navarathna, B. Wayne Bequette, Faye Cameron

Department of Chemical and Biological Engineering, Rensselaer Polytechnic Institute, Troy, 12180

contact: navarp@rpi.edu

Since 65% of adolescents with Type 1 diabetes in a study by Burdick et al. (2004) missed 1 or more meal insulin boluses in a week, automatically detecting meals would enable an advisory system to remind patients to bolus and predict future exercise. This work seeks to automate collecting patient logs using smart device based activity detection. We envision daily patient review to remove false positive detections. These detections are then used to forecast future activity.

Sleep, eating, and exercise were logged by three investigators while collecting data on a smartphone and smartwatch. An LSTM based neural network was trained on watch accelerometer and gyroscope data to classify other, sleep, eating, and exercise activities. Location data from the phone's GPS were used to generate a lookup table that returns activity probabilities given location. The outputs from these individual algorithms were combined with Bayes' rule. A particle filter is used to correct classifications over time (trend-correction) and forecast activity based on the most probable particle. Prior probabilities are determined using the American Time Use Survey (ATUS) as a population level dataset.

The classifier (real-time, minute based) correctly classified 78%/78.9%/87.8% of sleep/eating/exercise minutes. The classifier exhibits false positive rates of 15.1%/54.3%/77.8% with sleep/eating/exercise. The classifier's noise on logged data is used to simulate classifications on ATUS days and detect events over time through trend correction. After the course of a day 100%/ 98% /96.8% sleep/eating/exercise events are detected. The resulting false positive rates are 0.3%/0.5%/1.57% for sleep/eating/exercise. The particle based prediction is more accurate than prediction based on priors and prediction based on the continuity of the current activity.

Filtering real-time classification significantly improves detection accuracy. This accuracy level should be sufficient for activity automatic logging with daily patient review. Adapting priors to patients also reduces false positive identifications.

PP.01 ZHIPENG LI
12:45 – 1:45

Revealing the Excitonic Complexes Fine Structure in BN Encapsulated Monolayer WSe_2

Zhipeng Li[1,2], Tianmeng Wang[1], Zhengguang Lu[3,4], Chenhao Jin[5], Yanwen Chen[1], Yuze Meng[1,6], Zhen Lian[1], Takashi Taniguchi[7], Kenji Watanabe[7], Shengbai Zhang[8], Dmitry Smirnov[3], Su-Fei Shi[1,9]

1. Department of Chemical and Biological Engineering, Rensselaer Polytechnic Institute, Troy, NY 12180
2. School of Chemistry and Chemical Engineering, Shanghai Jiao Tong University, Shanghai, 200240, China
3. National High Magnetic Field Lab, Tallahassee, FL, 32310
4. Department of Physics, Florida State University, Tallahassee, Florida 32306, USA
5. Physics Department, University of California, Berkeley, CA 94720
6. College of Physics, Nanjing University, Nanjing, 210093, P. R. China
7. National Institute for Materials Science, 1-1 Namiki, Tsukuba 305-0044, Japan.
8. Department of Physics, Applied Physics, and Astronomy, Rensselaer Polytechnic Institute, Troy, NY 12180
9. Department of Electrical, Computer & Systems Engineering, Rensselaer Polytechnic Institute, Troy, NY 12180

contact: liz28@rpi.edu

Strong Coulomb interactions in single-layer transition metal dichalcogenides (TMDs) result in the emergence of strongly bound excitons, trions and biexcitons. These excitonic complexes possess the valley degree of freedom, which can be exploited for quantum optoelectronics. However, in contrast to the good understanding of the exciton and trion properties, the binding energy of the biexciton remains elusive, with theoretical calculations and experimental studies reporting discrepant results. In this work, we present the high-quality low-temperature photoluminescence (PL) spectra of BN encapsulated monolayer WSe_2, which directly reveals the biexciton state only exists in charge neutral WSe_2 and one free electron binds to a biexciton and forms the trion-exciton complex, the binding energy is ~17 meV and ~49 meV for biexciton and trion-exciton complex, respectively. The magneto-PL also reveals unambiguous evidence of the dark exciton. The improved understanding of the biexciton, trion-exciton complexes and other excitonic complexes improve our understanding of the many-body interaction in TMDs, promising novel application in low-dimensional quantum optoelectronics.

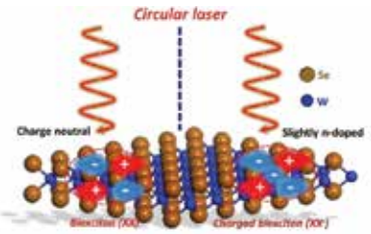

Acknowledgements: The device fabrication was supported by Micro and Nanofabrication Clean Room (MNCR), operated by the Center for Materials, Devices, and Integrated Systems (cMDIS) at Rensselaer Polytechnic Institute (RPI). We acknowledge the support from the Air Force Office of Scientific Research through Grant FA9550-18-1-0312 and the support from the US Department of Energy (DE-FG02-07ER46451) for magneto-photoluminescence measurements performed at the National High Magnetic Field Laboratory, which is supported by National Science Foundation through NSF/DMR- 1157490, NSF/DMR-1644779, and the State of Florida.

PP.02 PEIJIAO FANG
12:45 – 1:45

Growth of Cubic Epitaxial WC_{1-x}(001) Layers

Peijiao Fang, Baiwei Wang, Erik Milosevic, Daniel Gall

Materials Science and Engineering Department, Rensselaer Polytechnic Institute, Troy, NY 12180, USA

contact: fangp@rpi.edu

Epitaxial WC_{1-x}(001) layers are deposited on MgO(001) by reactive magnetron sputtering in a 5 mTorr CH_4 - Ar mixture at 400 °C. High-resolution x-ray diffraction ω-2θ scans, ω rocking curves and asymmetric reciprocal space maps indicate an epitaxial cube on cube relationship: $(001)_{WC}$ || $(001)_{MgO}$ and $[100]_{WC}$ || $[100]_{MgO}$. The rocking curve full-width at half-maximum of the WC_{1-x} 002 reflection is < 0.08° for all layers, suggesting an excellent crystalline quality. Increasing the CH_4 partial pressure from 0.05 to 1 mTorr leads to an increase in the measured relaxed lattice constant from 4.225 to 4.262 Å, indicating an increasing carbon concentration in the deposited layers. However, simultaneously, the vertical x-ray coherence length decreases from 19 to 4 nm, suggesting that surface segregated excess carbon may nucleate crystalline defects and/or misoriented grains. Atomic force microscopy (AFM) shows that the surface morphology exhibits 2-4 nm deep and 0.5-1.5 µm wide pits, leading to an overall root-mean-square (rms) roughness of 0.8±0.1 nm, in good agreement with 1.0±0.2 nm from x-ray reflectivity measurements.

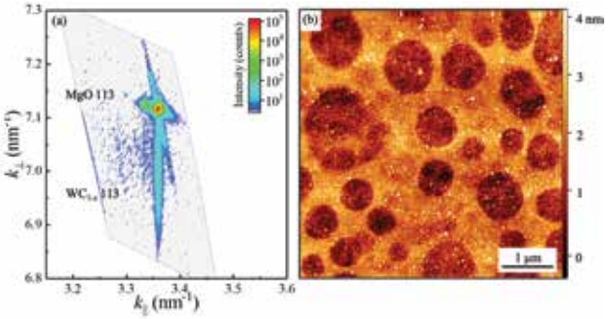

Figure 1: (a) X-ray diffraction reciprocal space map and (b) AFM micrograph from an epitaxial WC_{1-x}(001)/MgO(001) layer. The vertically aligned WC_{1-x} and MgO 113 reflections indicate a fully strained layer.

PP.03 ANNA SMALLWOOD

12:45 – 1:45

Chemical and Mechanical Analysis of Stereolithography 3D Printed Thermoset Polymer Networks

Anna Smallwood, Rykelle Adley, Chang Y. Ryu

Department of Chemistry and Chemical Biology, Rensselaer Polytechnic Institute, Troy, NY-12180

contact: smalla3@rpi.edu

Stereolithography (SLA) is a method of 3D printing in which objects are formed through the repeated curing of light-reactive photopolymer resin by a computer-controlled UV laser source. Morphology of SLA-printed objects is characterized by a layered structure on the microscopic scale. The crosslinking density of each layer as it is formed during printing is a function of the wavelength, intensity and UV penetration depth of the SLA printer's light source. Each layer is comprised of a stiff, highly crosslinked region that decays gradually into a more lightly crosslinked domain characterized by incomplete curing during printing. The thickness of each layer can be controlled between 25 and 200 micrometers, defined as the "slice thickness" of the SLA print. This layered morphology, coupled with printing orientation and slice thickness, has significant effects on the overall mechanical properties of SLA-printed objects.

SLA-printed object morphology will be investigated by high-resolution microscopy techniques such as scanning electron microscopy (SEM) while curing dynamics as a function of layer thickness will be studied through differential scanning calorimetry (DSC) and dynamic mechanical analysis (DMA).

PP.04 ZHIBO GUO

12:45 – 1:45

Pyroelectric Polarization Effect on the Electrical Properties of (0001) GaN MOS/MIS Interfaces

Zhibo Guo, Collin Hitchcock and T. P. Chow

Lighting Enabled Systems & Applications Center, Rensselaer Polytechnic Institute, Troy, NY 12180

contact: guoz3@rpi.edu

The pyroelectric effect describes the variation of polarization charges with changing temperatures in (0001) GaN. In this work, we have determined the pyroelectric temperature coefficient from flatband voltage (V_{FB}) variation with temperature on several (0001) GaN MOS/MIS capacitors, indicating the general nature of this phenomenon.

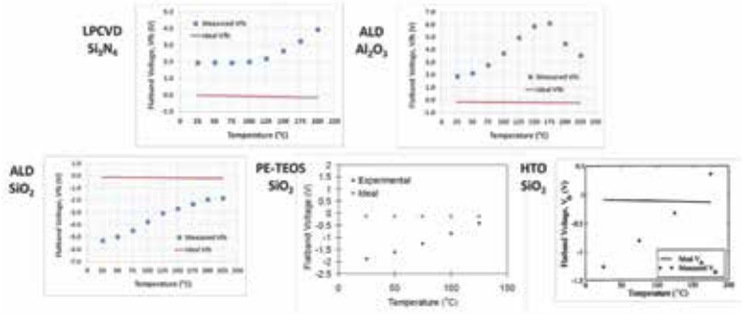

Figure. Measured flatband voltage vs. temperature compared with ideal flatband voltage.

Five GaN MIS capacitor samples were fabricated on unintentionally doped (UID) GaN epitaxial layers grown by MOCVD on sapphire substrates. One sample used LPCVD Si_3N_4, a second used thermal ALD Al_2O_3, and three others used SiO_2 deposited using three different techniques - plasma-assisted ALD, PECVD using TEOS, and high temperature oxide (HTO). Temperature-dependent capacitance-voltage (C-V) curves of the GaN MIS capacitors are measured. The flatband voltages are extracted and shown in the figure, indicating a positive flatband voltage shift with increasing temperature. This anomalous temperature dependence can be explained by the temperature dependent behavior of polarization charges. While Q_f is not expected to change with temperature, the expected decrease in the magnitude of the negative Q_{it} with temperature will tend to decrease V_{FB}. Additionally, the expected increase of Φ_s as the Fermi level moves towards midgap at higher temperatures should also shift V_{FB} to the left. Therefore, the positive V_{FB} shift at moderate temperatures can only be attributed to the increase in magnitude of the negative polarization charge Q_{pol}. In summary, the pyroelectric polarization effect of GaN was experimentally determined in Si_3N_4, Al_2O_3 and SiO_2 MIS capacitors.

Acknowledgements: This work was supported primarily by the Engineering Research Centers Program (ERC) of the National Science Foundation under NSF Cooperative Agreement No. EEC-0812056 and in part by New York State under contract C160145.

PP.05 ZHIBO GUO
12:45 – 1:45

Comparative Performance Evaluation of Lateral and Vertical GaN High-Voltage Power Field-Effect Transistors

Zhibo Guo, Collin Hitchcock and T. P. Chow

Lighting Enabled Systems & Applications Center, Rensselaer Polytechnic Institute, Troy, NY 12180

contact: guoz3@rpi.edu

We have evaluated specific on-resistance ($R_{on,sp}$) and switching performance of various GaN power field-effect transistors (FETs) with 600 V and 1200 V ratings using analytical calculations and numerical simulations. The normally-off GaN power FET family includes lateral p-GaN gate HEMTs, lateral MOS channel HEMTs, vertical CAVETs and vertical UMOSFETs. Their schematic cross-sections are shown in the figure.

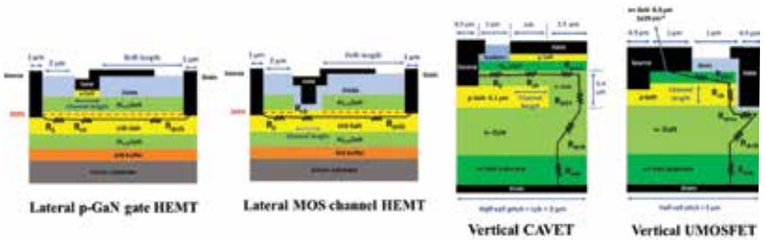

Schematic cross-sections with on-state resistance components of GaN power FETs

$R_{on,sp}$ of different devices are calculated and compared. $R_{on,sp}$ is primarily determined by two key factors: vertical vs. lateral topology, and MOS channel vs. 2DEG channel. As a combination of vertical topology and 2DEG channel, CAVETs show smallest $R_{on,sp}$. UMOSFETs are second only to CAVETs. At the 600 V rating, $R_{on,sp}$ of UMOSFETs and p-GaN gate HEMTs are comparable, while at the 1200 V rating, the advantage of vertical topology manifests and $R_{on,sp}$ of the UMOSFET is only half that of the p-GaN gate HEMT. Device-circuit mixed-mode simulations incorporating inductive and resistive load circuits are used to predict switching time and energy loss, which correlate with the $R_{on}*Q_G$ figure-of-merit as well as gate voltage swing. For devices of 600 V rating, results show that larger $R_{on}*Q_G$ corresponds to larger Etotal and longer toff. Vertical devices have larger Q_G than lateral HEMTs. UMOSFETs outperform MOSC-HEMTs due to substantially lower $R_{on,sp}$, even though $Q_{G,sp}$ is worse. At the 600 V rating, P-GaN gate HEMTs and CAVETs switch faster and with lower loss than UMOSFETs owing to their smaller $R_{on}*Q_G$. For 1200 V devices, UMOSFETs outperform p- GaN gate HEMTs and are comparable to CAVETs due to improvement in $R_{on}*Q_G$ relative to the 600 V rating. Although p-GaN gate HEMTs still have lower $R_{on}*Q_G$ than UMOSFETs, their smaller VGS swing negates this advantage. This study shows the advantages of vertical GaN power FETs over lateral GaN power HEMTs at higher voltage ratings (1200 V). At moderate (600 V) ratings, P-GaN gate HEMTs are as competitive as vertical devices.

Acknowledgements: This work was supported primarily by the Engineering Research Centers Program (ERC) of the National Science Foundation under NSF Cooperative Agreement No. EEC-0812056 and in part by New York State under contract C160145.

PP.06 ZHIBO GUO
12:45 – 1:45

Monolithic Optoelectronic Integration of GaN Quasi-vertical UMOSFET and LED

Zhibo Guo, Collin Hitchcock and T. P. Chow

Lighting Enabled Systems & Applications Center, Rensselaer Polytechnic Institute, Troy, NY 12180

contact: guoz3@rpi.edu

Monolithic optoelectronic integration of GaN light-emitting diode (LED) and GaN driving field-effect transistor (FET) holds considerable promise in the application of visible light communication (VLC). Compared with hybrid-packaged FET/LED pairs, monolithic integrated FET/LED pairs are compact, cost-effective, and eliminate parasitic inductance and resistance in FET/LED interconnections, enabling faster switching and hence higher data transmission rates in VLC. In this work, we experimentally demonstrated GaN quasi-vertical UMOSFET/LED integration using selective epi removal (SER) approach.

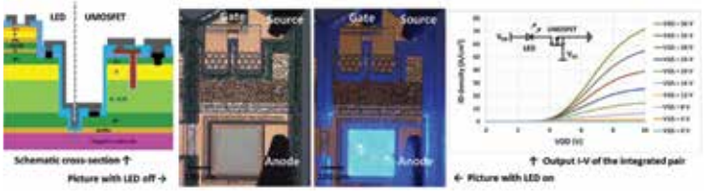

Fabrication started on the MOCVD-grown GaN-on-sapphire wafer, with LED epi on top of n/p/n FET epi. LED epi was selectively etched away in the FET area first, followed by gate trench, body trench, drain trench and isolation trench etching, as well as gate oxide and polysilicon deposition. After inter-layer dielectrics (ILD) deposition, source/cathode/drain and anode contacts were evaporated and annealed. The process was finalized by sputtered Ti/Al for both FET/LED interconnects and probing pads. The LED anode contact was protected by a thin oxide layer during wet-etch patterning of Ti/Al. The metal-oxide-semiconductor-gated channel on p-GaN works in normally-off mode, which is desirable for false-safe operation and simplification of gate driver design. The LEDs emit blue light with size as small as 100-200 μm, which is typical for LED display applications. The output I-V of integrated series-connected UMOSFET/LED was measured by sweeping supply voltage VDD at different gate voltage VGS, showing a full modulation of LED current and light output by gate voltage. This demonstrates compatibility of GaN UMOSFET and GaN LED processes, and creates a new technology platform for GaN optoelectronic integration for a variety of smart-lighting applications.

Acknowledgements: This work was supported primarily by the Engineering Research Centers Program (ERC) of the National Science Foundation under NSF Cooperative Agreement No. EEC-0812056 and in part by New York State under contract C160145. The fabrication in this work makes extensive use of cleanroom facilities in the Center for Materials, Devices and Integrated Systems (cMDIS) at RPI.

PP.07 GENEVIEVE KANE
12:45 – 1:45

Control of Ti-6Al-4V using Adaptive Microscale Simulator techniques

Arun Baskaran,[1 b] Sagar Bhatt,[2 b] Zhenhan Huang,[1b] Genevieve Kane,[4 b] Michael Allahua,[2 c] Dan Lewis,[1 a] Antoinette Maniatty,[2 a] John Wen,[2 ,3a] Robert Hull[1 a]

1 Department of Materials Sci and Eng, Rensselaer Polytechnic Institute, Troy, 12180
2 Department of Mechanical, Aerospace & Nuclear Eng, Rensselaer Polytechnic Institute, Troy, 12180
3 Department of Industrial & Systems Eng, Rensselaer Polytechnic Institute, Troy, 12180
4 School of Engineering, Rensselaer Polytechnic Institute, Troy, 12180

a Faculty, b Graduate students, c Undergraduate student

contact: kaneg@rpi.edu

Ti-6Al-4V is a dual-phase alloy, used mainly in aerospace and biomedical applications owing to its high specific strength, excellent high temperature properties, and corrosion resistance. In support of the Materials Genome Initiative, a collaborative effort combining simulation, experimental and feedback control has been created to allow for enhanced material manufacturing at a lower cost. To achieve this, an adaptive microscale simulator (AMS) is being developed to examine the relationship between thermomechanical processing conditions and microstructure evolution. This approach allows for real-time control of microstructure using a scanning electron microscope with in situ tensile testing and nano-indentation stages coupled with the use of feedforward and feedback control. Modeling of microstructure evolution using Monte-Carlo (MC) methods, finite element crystal plasticity, and microelasticity theory augmented phase field method help to interpret experimental results, and inform the processing conditions for design of future experiments.

We are able to establish a "library" of Ti-6Al-4V alloy microstructures resulting from a variety of deformation and heating conditions to inform initial simulations. Grain boundaries can be detected and compared to human tracings to automatically detect microstructure during real-time testing. These can be used in the MC grain growth code, calibrated using literature data, to predict temperature driven grain structure evolution and can simulate BCC β-phase grain growth. A simple hybrid Potts-phase field model provides a framework to model grain growth below β-transus. Simulated FEM and experimental data are compared with development of initial FEM/MC suite as the goal. Augmentation of crystallographic symmetry and α-β orientation relationship into a phase field model has enabled us to model the growth of twelve unique α variants. Currently, work a multi-phase formalism is being developed to model the influence of processing conditions on the strain-driven preferential variant selection of α variants or lack thereof.

Acknowledgements: This research is sponsored through a grant from the National Science Foundation, Award CMMI-1729336, DMREF: Adaptive control of Microstructure from the Microscale to the Macroscale

PP.08 ARUN BASKARAN
12:45 – 1:45

A supervised learning method to classify titanium alloy microstructures and quantify morphological features

Arun Baskaran

1 Department of Materials Sci and Eng, Rensselaer Polytechnic Institute, Troy, 12180

contact: baskaa2@rpi.edu

An image driven supervised learning method has been implemented on dual phase titanium alloy microstructures for learning and quantification of important morphological features such as equiaxed α, α laths, orientation distribution of α laths, etc. Subsequently, these microstructures were classified based on the dominant morphological feature. The alloys in consideration, for example Ti-6Al-4V, exhibit a wide variety of meso-scale morphologies influenced by factors such as crystal symmetry, orientational relationship between the phases, processing condition, alloy history, etc. Subtle changes in the microstructure measurably affect the physical properties of the material, and hence it is important to quantify the dominant morphological features. For this study, the training and test datasets are built from a database of optical and SEM micrographs, consisting of roughly 400 images. Due to the varying nature of the micrographs, all the images were pre-processed before training. The project has been completely implemented on the Python 3.0 platform with the aid of libraries scikit-learn and imgaug, the former for importing classification methods and the latter for pre-processing and normalization. The learning method involves training a Support Vector Machine on independent features of the training images, such as grayscale histograms, average pixel intensity, area fraction of boundary regions, etc. The primary classification target was to label the microstructures as lamellar and equiaxed. Subsequently, the lamellar label was expanded into two labels and the images were classified as equiaxed, basket-weave, or colony, depending on their dominant feature. Quantitatively decomposing such complex microstructures into its dominant morphological features will aid in further bridging the gap in its processing-structure-property relationships.

Acknowledgements: This project was undertaken as part of the coursework, Material Informatics and Data Science (MTLE6960).

PP.09 DING TIAN
12:45 – 1:45

Synthesis and Characterization of Anion Exchange Membrane via Simultaneous Post-functionalization and Crosslinking of Epoxidized SBS

Ding Tian[1], Chang Y. Ryu[1], Chulsung Bae[1,2]

1 Department of Chemistry and Chemical Biology, Rensselaer Polytechnic Institute, 110 8th Street, Troy, NY 12180, United States

2 Department of Chemical and Biological Engineering, Rensselaer Polytechnic Institute, 110 8th Street, Troy, NY 12180, United States

contact: tiand@rpi.edu

Anion exchange membrane fuel cell (AEMFC) has been recognized as a potential alternative to the high-cost proton exchange membrane fuel cell (PEMFC) due to its possibility to use non-precious metal catalyst and faster kinetics of cathode reaction. However, a wider commercialization of AEMFC is restricted by a few challenges including a lack of satisfactory anion exchange membrane which has good conductivity, alkaline stability, mechanical property, and scale-up capability. In this presentation, we report a simultaneous post-functionalization and crosslinking approach for polystyrene-*b*-polybutadiene-*b*-polystyrene (SBS) triblock copolymer using photo-initiated cationic polymerization. Controlled amount of oxiranes were introduced to the polybutadiene block of SBS followed by blending with alkyl bromide-substituted oxirane additives and photoacid generator. The cationic oxirane ring-opening polymerization was initiated under UV irradiation, rendering crosslinked polymer network tethered with alkyl bromide side chains. The bromide group was eventually replaced to quaternary ammonium functional group by nucleophilic substitution to offer anion conductivity. Our synthetic work was successfully confirmed by FT-IR and titration. The resulting crosslinked polymer membrane exhibited ion exchange capacity (IEC) of 1.5 mmol/g with hydroxide conductivity of 85 mS/cm at 80 °C and 100% relative humidity (RH). Mechanical property was characterized by tensile test using dynamic mechanical analysis under 50 °C and 50% RH. Compared with pristine SBS, the tensile strength was improved by 200% while elongation at break higher than 150% can still be maintained (Fig 1). Because of flexible, efficient, tunable, and low-cost nature of our synthetic approach, it will offer a new synthetic platform for the generation of mechanically robust anion exchange membrane materials for fuel cell applications.

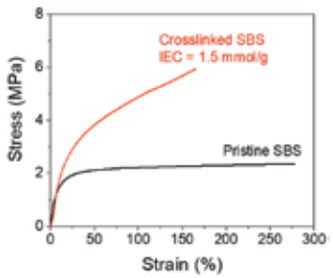

Figure 1. Stress-strain behavior change upon crosslinking of SBS

Acknowledgements: This work is supported by National Science Foundation (DMR 1506245)

PP.10 COLIN DANIELS
12:45 – 1:45

Scalable Calculations of Raman Spectra and Application to Carbon Nanotube Coils

Colin Daniels[1], Michael Lamparski[1], Vincent Meunier[1]

1 Department of Physics, Rensselaer Polytechnic Institute, Troy, New York 12180, USA

contact: daniec4@rpi.edu

In many fields, including materials science and condensed matter physics, Raman spectroscopy is a powerful non-destructive technique for the characterization of samples produced experimentally. Due to the underlying physics of Raman scattering, the data obtained from Raman spectroscopy can be used to give significant insight into the structure of a material. The theoretical approach to generating a Raman intensity spectrum traditionally involves the use of density functional theory to calculate the forces and material polarizability needed for the calculation of intensities, but this has scaling problems for larger systems.

An alternative method is discussed for calculations involving carbon-based nanostructures and materials. This method combines a bond-polzariability based approximation with force fields normally used in molecular dynamics simulations, such as ReaxFF or AIREBO. In par- ticular, the theoretical Raman spectra of defect-free carbon nanotube coils, which have recently been produced experimentally, are calculated with this model. The changes in the low fre- quency phonon modes due to van der Waals interactions between the nanotubes in the coil are then examined, along with the related effects tied to finite coil diameter and nanotube chirality.

PP.11 SAMBIT GOSH
12:45 – 1:45

Using Cognitive Computing for the Control Room of the Future

Sambit Ghosh, B. Wayne Bequette

Department of Chemical and Biological Engineering, Rensselaer Polytechnic Institute, 110 Eighth Street, Troy, NY 12180, USA

contact: ghosh3@rpi.edu

Chemical manufacturing processes are often complex and large-scale, with many variables to monitor and control. The start-up and shutdown of process units can be particularly challenging, with specific and coordinated sequences of events to assure safety while completing operation goals in a reasonable amount of time. The inclusion of human-in-the-loop manual control makes the process more challenging. As a result, tools for including and analysing humans and process equipment together are required.

Recent advances in cognitive computing, "big data" and process data analytics have great potential to improving the transient operation of chemical processes with human-in-the-loop. A framework to study process start-ups, shutdowns and abnormal events using graph theory, cognitive computing and machine learning is presented. Preliminary results based on a simple two-tank problem show the usefulness of graph-based analyses. Deviations in the start-up protocol and a sensor fault are detected using this procedure. Ongoing research tests the proposed strategy on more realistic larger scale chemical processes and with closed-loop control.

PP.12 YUEMING XU
12:45 – 1:45

The Development of the Charge Transport Model to Predict Dielectric Failure

Yueming Xu[1], Joel L. Plawsky[1], Toh-Ming Lu[2]

1 Howard P. Isermann Department of Chemical and Biological Engineering, Rensselaer Polytechnic Institute, Troy, 12180,

2 Department of Physics, Rensselaer Polytechnic Institute, Troy, 12180

contact: xuy18@rpi.edu

A charge transport model was previously developed in our group to predict intrinsic dielectric failure as a function of voltage for low-k SiCOH and high-k SiN, two materials commonly used in integrated circuits. The model incorporates a set of fundamental mechanisms, including electronical conduction and defect generation, resulting in breakdown when a critical defect density is reached. It replicated electrical conduction through dielectric materials and so can describe the entire history of current flow through the dielectric. Furthermore, a revised version of this model was recently proposed, and it overcame two limitations of the original model: the lack of thickness and temperature dependence. One issue recently investigated was the assumption that the effective velocity of tunneling electrons was the same as mobile electrons. These velocities are used to calculate the electron flux/current. New models separating the two velocities were developed and to fit the experimental data. These newer models offered slightly worse reliability predictions, and so the initial assumption remains not only simpler, but also more accurate so far. This model will be applied to predict the filament formation in resistive switching memory devices.

PP.13

BAIWEI WANG
12:45 – 1:45

Fully Strained Epitaxial $Ti_{1-x}Mg_xN$/MgO(001) Layers Grown by Reactive Magnetron Sputtering Deposition

Baiwei Wang and Daniel Gall

Department of Materials Science and Engineering, Rensselaer Polytechnic Institute, Troy, NY 12180, USA

contact: wangb12@rpi.edu

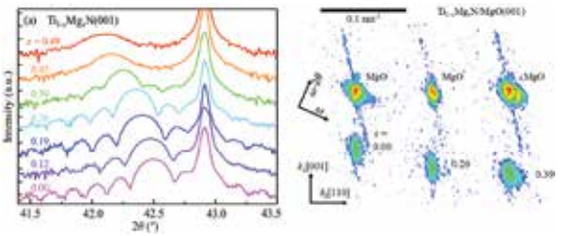

The goal of this research is to investigate the interdependence of strain relaxation with thickness and composition for $Ti_{1-x}Mg_xN$ layers, which is a promising new material system for semiconducting (x = 0.5), thermoelectric and plasmonic devices, without compromising its refractory and CMOS-compatible properties. Single crystal $Ti_{1-x}Mg_xN$(001) layers (0.00 ≤ x ≤ 0.49) were deposited on MgO(001) by reactive magnetron co-sputtering from titanium and magnesium targets in 5 mTorr pure N_2 at 600 °C. X-ray diffraction ω-2θ scans, ω-rocking curves, φ-scans, and high resolution reciprocal space maps show that rock-salt $Ti_{1-x}Mg_xN$ layers are epitaxial single crystals with a cube-on-cube epitaxial relationship with the substrate: $(001)_{TiMgN}||(001)_{MgO}$ and $[100]_{TiMgN}||[100]_{MgO}$. $Ti_{1-x}Mg_xN$(001) layers, with thickness 36 nm ≤ d ≤ 57 nm, are fully strained after deposition, yielding an in-plane lattice parameter $a_{||}$ = 4.212 ± 0.001 Å and out-of-plane lattice parameters a□ that increase from 4.259 Å (x = 0.00) to 4.289 Å (x = 0.49), following a bowing expression a□ = (1-x)a_{TiN} + xa_{MgN} – bx(1-x), where a_{TiN}, a_{MgN}, and b are fitting parameters determined as 4.255, 4.432, and 0.199 Å, respectively. The in-plane x- ray coherence length $\xi_{||}$ is large, 156-381 nm, for 0.00 ≤ x ≤ 0.45, but drops to 25 nm for x = 0.49, indicating local strain variations and a considerable reduction of the distance between threading and/or misfit dislocations when the alloy approaches phase separation. The out-of-plane x-raycoherence length ξ□ matches the layer thickness. $Ti_{1-x}Mg_xN$(001)layerswithalarger thickness (110 nm ≤ d ≤ 275 nm) exhibit a mild compressive strain (-0.34% for pure TiN) or are fully relaxed (for alloys), indicating a thickness-induced strain relaxation.

PP.14

TRAVIS DIAMOND
12:45 – 1:45

Prediction of Postprandial Glycemic Response from Meal Models of Varying Complexity

Travis Diamond, B. Wayne Bequette, Faye Cameron

Department of Chemical and Biological Engineering, Rensselaer Polytechnic Institute, Troy, 12180

contact: diamot@rpi.edu

In individuals with type 1 diabetes, meals act as a consistent disturbance to blood glucose (BG) control. Glucose from meals raises blood sugar, which requires the patient to inject insulin to compensate. In artificial pancreas (AP) systems, the burden of controlling BG is handled automatically. A continuous glucose monitor (CGM) measures subcutaneous glucose (SG) to inform a control algorithm. A control algorithm often used is model predictive control (MPC), which uses a model of the glucose-insulin system, combined with current SG measurements, to predict the BG trajectory. The prediction is used to calculate how much insulin to deliver, which is handled by an insulin pump attached to the patient.

Our work aims to develop an improved meal model for the AP control algorithm. A meal model describing the rate of glucose appearance from foods commonly eaten can improve predictions and provide better BG control during the postprandial period. The meal model must be able to fit different glucose appearance curves from triple-tracer (TT) studies, the gold standard technique for measuring rate of meal glucose appearance in the blood stream. The model should also be able to predict the total meal glucose using CGM readings taken after meal ingestion, and update the prediction as new readings are obtained.

Seven meal models of various complexities were developed, and least squares fits were done for 25 meal shapes obtained using the TT technique. A model designed from the physiology of glucose digestion fit the TT meal shapes with the least error. To evaluate the model's ability to predict, Kalman-filtered predictions of total meal glucose were made every 5 minutes using data from the first 60 minutes of each triple tracer study. A nonlinear model, composed of a weighting scheme between two curves, was found to provide the most accurate predictions of total meal glucose.

PP.15 MARC-ANTOINE FORTIN
12:45 – 1:45

The Isotope Mass Effect on the Diffusion of Volatile Elements in Silicate Melts

Marc-Antoine Fortin[1], E. Bruce Watson[1], Richard A. Stern[2], Shuhei Ono[3]

1 Department of Earth and Environmental Sciences, Rensselaer Polytechnic Institute, Troy, 12180,
2 Canadian Centre for Isotopic Microanalysis, University of Alberta, Edmonton, Canada, T6G 2E3,
3 Department of Earth, Atmospheric, and Planetary Sciences, Massachusetts Institute of Technology, Boston, 02139

contact: fortim@rpi.edu

The isotopic signatures of volatile elements have been used extensively as geochemical tools in Earth science, and kinetic effects have been linked to fractionations in silicate melts. Owing to their mass difference, the diffusivities of individual isotopes are expected to differ slightly. This isotope mass effect on diffusion is a potentially significant control on the isotopic signatures of natural systems. Here, we present an experimental study of this effect on stable isotopes of Cl and S—two geologically-important volatile elements.

This is achieved using a piston-cylinder apparatus to generate dry, synthetic quenched melts under geologically-relevant conditions, between 1200 and 1350 °C at 1 GPa. In this apparatus, atoms of Cl or S are induced to diffuse from one half of the experiment to the other. Initially, in both halves, the major element compositions and the isotopic signatures are the same, but the concentrations of the element of interest are such that there is a chemical gradient in Cl or S. The experiment run products were analyzed by secondary ion mass spectrometry and isotope ratio mass spectrometry.

We report a ratio of diffusivities for $^{37}Cl/^{35}Cl$ of 0.994±0.001. In contrast to previously- characterized isotopes, we find no significant isotope mass effect on the diffusivities of ^{32}S and ^{34}S. We suggest that this can be explained by the complexation of S species with heavier elements in the melt (e.g., FeS), which effectively weakens the mass effect.

PP.16 YING ZHANG
12:45 – 1:45

Modeling chloride diffusion in concrete: a coupled multi-physics formulation

Ying Zhang, Mohammed Alnaggar

Civil and Environmental Engineering, Rensselaer Polytechnic Institute, Troy, 12180

contact: zhangy61@rpi.edu

The chloride-induced corrosion of reinforcement is one of the most important reasons that cause serious deterioration of the infrastructure. According to current statistics, one out of nine bridges in the United States is rated as structurally deficient and 20% of the repair costs are directly due to corrosion. For better durability design and prediction, a reliable and applicable calculation method for chloride penetration in concrete is necessary.

Chloride transport through cement-based materials is different from that in an infinite dilute solution because of the complicated microstructure and chemical reactions in concrete. Many exist methods are simply based on chloride diffusion in dilute solution and then experimentally fitted. This methodology didn't combine the diffusion process with the material properties of concrete at microstructural level, and therefore failed to theoretically explain the significant influences of the cementitious media and didn't fully capture the main features of chloride diffusion in concrete pore solution.

This study intends to develop a coupled multi-physics simulation method for chloride diffusion in concrete. The impact of concrete material on diffusion is stressed in the model on two aspects: the membrane effect and the pore structure. As is well known, the matrix performs as an electronegative permeable membrane. The proposed model considers this phenomenon by membrane potential, which actually accelerate the anions to maintain macroscopic electrical neutrality. The binding capacity of the matrix is described by the Freundlich law and coupled with the hydration process. Other than that, the diffusivity in pore solution is described by considering tortuosity and porosity related to the aging of concrete. Also, temperature effects are automatically captured through the Arrhenius-type dependence of diffusivity and binding capacity on temperature. The modelling parameters are carefully calibrated by the test results and excellent agreement is observed in predicting the chloride profile in concrete.

PP.17 YUEH-TING SHIH
12:45 – 1:45

The Structural Origin of the Anomalous Density Maximum in Silica and Alkali Silicate Glasses

Yueh-Ting Shih[1,2] and Liping Huang[1]

1 Department of Materials Science and Engineering, Rensselaer Polytechnic Institute, Troy, NY 12180, United States

2 Department of Materials Science and Engineering, National Tsing Hua University, Hsinchu, Taiwan

contact: shihy2@rpi.edu

Silica, sharing the same tetrahedral order and many structural, thermodynamic and dynamic anomalies with water, has been speculated to have density increase upon melting similar to water. In this work, a density increase upon melting cristobalite silica and a shallow density maximum during cooling of silica liquid are observed in classical molecular dynamics (MD) simulation. The density maximum gradually diminishes with the increase of alkali size/content in alkali silicate glass. The structural origin of the anomalous density maximum is revealed by detailed structural analysis in MD simulation. During the cooling process, the liquid silica tends to transform to the crystalline cristobalite, which consists of 6-member rings that give a more open structure and a lower density than the liquid. However, due to the high viscosity of silica liquid, long range order in cristobalite cannot form, but 6-member rings still predominate, which cause the silica network to open up and compensate the regular volume shrinkage upon cooling. These two competing factors lead to a density maximum, but to a less extent than that observed in melting cristobalite. With the increase of modifier size/content in the alkali silicate glass, the connection of silica network gradually breaks down; the population of 6-member rings decreases with the increase of smaller or larger rings, therefore the density maximum becomes less obvious and eventually disappears.

PP.18 XIANGYU GONG
12:45 – 1:45

Large-scale patterning of single cells and cell clusters in hydrogels for studying tumor progression

Xiangyu Gong[1,2], and Kristen L. Mills[1,2]

1 Department of Mechanical, Aerospace, and Nuclear Engineering, Rensselaer Polytechnic Institute, 110 8th St, Troy, NY 12180

2 Center for Biotechnology and Interdisciplinary Studies, Rensselaer Polytechnic Institute, 110 8th St, Troy, NY 12180

contact: gongx@rpi.edu

In the quest to understand the effects of the biophysical microenvironment on solid tumor progression, in vitro tumor models are important tools. Traditional two-dimensional (2D) cell culture does not accurately recapitulate tumor microenvironment (TME). To capture the properties of TME, three-dimensional (3D) models based on embedding tumor cells in hydrogels are often used. These models are additionally able to provide more relevant interactions between tumor cells and their environment. Random cell embedding, however, does not allow for spatial control over soluble or mechanical signals between cells, or long-term observation of tumor progression in an efficient fashion. Here we present an easy and low-cost method for large-scale, longitudinal studies of heterogeneous cell behavior in 3D hydrogel matrices. Using a platform we term "the drop- patterning chip", thousands of cells were simultaneously transferred from microwell arrays and fully embedded, only using the force of gravity, in precise patterns in 3D collagen I or Matrigel. This method allows for throughputs approaching 2D patterning methods that lack phenotypic information on cell-matrix interactions, and does not rely on special equipment and cell treatments that may result in a proximal stiff surface. With a large and yet well-organized group of cells captured in 3D matrices, we demonstrated the capability of locating selected individual cells and monitoring cell division, migration, and proliferation for multiple days. The flexibility of controlling the cell patterns in various hydrogel compositions may provide a powerful tool for in vitro studies of cell-cell interaction and tumor progression at the single-cell level.

PP.19 LIWEN CHEN
12:45 – 1:45

Non-equilibrium Close-Packed Block Copolymer Micelles

Liwen Chen, Sangwoo Lee

Department of Chemical and Biological Engineering, Rensselaer Polytechnic Institute, Troy, 12180

contact: chen115@rpi.edu

Close-packed structures are the fundamental crystal symmetries in nature, but the selective access to them has still remained as challenges. Block copolymer micelles are versatile model spherical particles in the investigation of self-assembling structures of spherical particles and associated phase transformation phenomena. We investigated the close-packed structures of spherical poly(butadiene-b-ethylene oxide) (PB-PEO) diblock copolymer micelles dispersed in water using synchrotron X-ray scattering measurements. Remarkably, rapid thermal quenching of disordered PB-PEO micelle solutions to different temperatures induced three representative close-packed structures: face-centered cubic (fcc), random stacking of 2-dimensional hexagonal close-packing (rhcp), and hexagonal close-packing (hcp). Careful examination of the 2- dimensional scattering patterns revealed that the clear correlation between the type of close- packed structures and the size of crystallites controlled by the depth of thermal quenching: the smallest crystallites stabilize hcp, and as the size of crystallites increases, the hcp transforms to rhcp and eventually settled to fcc. This observation shows the interfacial tension effect is crucial for the selection of the metastable crystal structures confined in small crystallites.

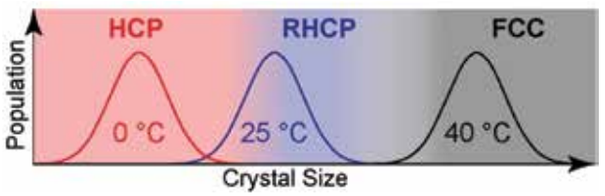

PP.20 SASIDHAR POTUKUCHI
12:45 – 1:45

Failure Mechanisms in Cortical Bone Microstructures during Fracture Cutting – Acoustic Emissions and Finite Element Modeling

Sasidhar Potukuchi[1], Roshan Mishra[1], Catalin Picu[1], Johnson Samuel[1]

1 Mechanical, Aerospace, and Nuclear Engineering Department, Rensselaer Polytechnic Institute, Troy, NY, 12180

contact: potuks@rpi.edu

Human bone microstructure changes with age, becoming more brittle and prone to thermal necrosis during orthopedic surgeries. To design patient-specific tooling to suit different microstructures seen in bone, failure mechanisms of the individual microstructural components must be explored. In this regard, novel fracture-monitoring methods like Acoustic Emissions (AE), combined with Finite Element tools like Cohesive Zone Modeling (CZM) provide inexpensive methods to model the failure mechanisms in bone. Furthermore, this combination can be employed to study the fracture behavior of materials with inseparable microstructures.

Therefore, the objectives of this research are, (1) to identify AE energies of the observed failure mechanisms in orthogonal machining of cortical bone and (2) to use the AE energies to estimate fracture energies of the microstructures which can be used as inputs to the CZM of the failure mechanisms.

For objective (1), orthogonal machining tests were performed on haversian and plexiform bone types with a 20° rake tool, observed with a high-speed camera, and the AE and cutting force signals were captured. The AE signals were mapped to the camera images to identify six distinct failure mechanisms. The acoustic energies per unit fracture area were calculated for each failure mechanism, showing the potential of this method for in-process monitoring of a surgical procedure.

For objective (2), CZM was used to simulate the observed failure mechanisms. The acoustic energies per unit fracture area obtained above were used to estimate the fracture energies of the microstructures. Cohesive tractions were 'tuned' so that the required failure mechanisms were simulated and the force per unit crack area from simulations matched the experimental outputs. The CZ models were validated using independent experimental data from orthogonal machining with a 0° rake tool. The validated CZ models were used to study the rake angle effects on the failure mechanisms and surface roughness.

PP.21 MOHAMMED ABDELLATEF

12:45 – 1:45

Interlocking plastic bottles as a structural building block

Mohammed Abdellatef[1], Mohammed Alnaggar[1]

1 Department of Civil and Environmental Engineering. Rensselaer Polytechnic Institute, Troy, NY, 12180

contact: alnagm2@rpi.edu

The use of recycled and sustainable building materials is one of the emerging topics in civil engineering. A recently patented innovative interlocking plastic bottle design is being investigated for possible use a building material for shelters during disaster relief situations. Immediately after disasters occur, huge supplies of water, drinks and food in plastic packaging is sent to the location. Getting red of the empty packaging becomes an environmental concern afterwards. If the supplies are sent in these bottles, then they are used to build transitional shelters, the environmental problem will be solved. In order to understand the mechanical behavior of a shelter made from these bottles, an extensive experimental program is performed.

A single bottle has an octagonal cross section measuring 5 cm in diameter and 10 cm in height. The bottles connect with each other via dovetail interlocking patterns on their sides. The program in this study consists of a series of experimental tests carefully designed to understand local and global behavior of the system. Tests included: single bottle behavior in compression, shear and interlocking, bending behavior of bottle assemblies with post-tensioned steel cables, and axial-compressive behavior of column assemblies. Different structural members were made including beams, roofs, columns and frames. A generalized global buckling of the column assemblies is obtained from fitting axial testing results of different column lengths and cross- sections. In addition, it was found that the bending capacity of beam assemblies is directly related to the shear/interlocking characteristics of the individual bottles. Based on this observation, bottle interfaces at beam ends were filled with expanding foam that provided a much higher load carrying capacity by arresting the interlayer slip mechanism. With these findings, the authors built a frame structure that represents 1⁄4 of a full shelter and presented it in the New York 2018 Maker Faire along with collaborators from the school of architecture and the Center for Architectural Science and Ecology (CASE) at Rensselaer. The built frame resisted the open site winds without any bracing for 3 days.

In conclusion, the interlocking plastic bottles show promising behavior as a new sustainable building material for transitional shelters during disaster relief.

Acknowledgements: The authors would like to acknowledge the support from Friendship Products LLC , and the participation from graduate (Shady Gomaa) and undergraduate students (Madelyn Babic, Chris Dearie, Tim Haddad, Alison Heisler, Carly Nadler, Jack Palmeri)

PP.22 CHRISTOPHER HOFF

12:45 – 1:45

Defect Thermometry and the Example of Al-in-Rutile

Christopher Hoff[1], Bruce Watson[1], Frank Spear[1]

1 Earth and Environmental Sciences, Rensselaer Polytechnic Institute, Troy, 12180

contact: hoffc@rpi.edu

The defect structure of rutile (TiO_2) is of considerable interest in materials science and geology. Rutile behaves as an n-type semiconductor and under reducing conditions deviates substantially from stoichiometry. Rutile is used as a detector material and has recently been discovered to be capable of colossal dielectric permittivity through coupled cation doping. Geologists are interested in rutile's defect structure because it directly reflects the nature of a rutile crystal's crystallization conditions. If the defect structure of rutile can be completely characterized, useful information about the temperature, pressure, and chemical environment of individual rutile crystals can be parsed out through careful analytical work.

To this end, we have experimentally investigated the solubility of aluminum in rutile as a function of temperature, pressure, and oxygen fugacity using high pressure-high temperature experimental techniques. Our rutile crystals were doped with varying 3+ and 5+ cations along with rutile to investigate their effect on aluminum solubility. The experimental products were rutile crystals generally 10's of μm in diameter and were measured using WDS on a Cameca SX 100 microprobe at RPI.

We found that the solubility of aluminum increases with temperature, pressure, oxygen fugacity, and Nb content. Our results are the first to show an increase in the solubility of aluminum with oxygen fugacity and we hypothesize therefore that aluminum is likely charge compensated with oxygen vacancies. We show that high pressure synthesis of rutile crystals makes it possible to elevate Nb^{5+} and Al^{3+} coupled substitution without the introduction of phase separation. For geological applications, we have shown that aluminum measurements on single crystals of rutile can return the temperature and pressure of rutile crystallization.

PP.23 JAMES NOVAK
12:45 – 1:45

A Data Science Approach to the Selection of Droplet Ejection Waveforms Used in Inkjet Printing

James Nowak[1], Hao Zhong[2], Peter Fox[2], Johnson Samuel[1]

1 Mechanical, Aerospace, and Nuclear Engineering Department, Rensselaer Polytechnic Institute, Troy, NY, 12180
2 Tetherless World Constellation, Rensselaer Polytechnic Institute, Troy, NY, 12180

contact: nowakj2@rpi.edu

Inkjet printing is a micro-scale additive manufacturing process that is utilized in applications such as the manufacturing of sensors and actuators, bio-printing of hydrogels, and binder-jet ceramic printing. The process produces droplets using an electric waveform to induce a vibratory motion in a piezoelectric crystal. The selection of an appropriate waveform for a given ink, is a time-consuming trial-and-error process, that is highly dependent on the fluid properties of the given ink. Inaccuracies in the waveform selection can result in either (i) no ejection of the droplet or (ii) droplets which break up upon exiting the nozzle. One possible approach to alleviate this is the use of data science and analytics to predict parameters (shape, amplitude, and period) of the waveform that could provide good quality droplets for a given ink.

In this work, we develop an approach of using data science tools to predict the waveforms of inks with differing fluid properties. First, a knowledge map is generated to allow for graphing of relevant process inputs and outcomes. Then, a series of experimental trials are performed to measure the droplet diameter and velocity across four training inks using different waveforms parameters.

Using the data from these training inks, decisions could be made on ejection parameters. First, for a given ink, the probability of a good quality droplet based on the shape of the waveform was determined. Then, a processing window, based on the Weber number, was identified. Finally, for a given ink and waveform shape, regression models were used to determine specific parameters (i.e. amplitude and period) for the waveform based on the processing window. These regression models were validated across four validation inks, to show efficacy in being able to predict appropriate trigger waveforms using this approach.

PP.24 RUFENG MA
12:45 – 1:45

Mechanosensing and force generation of healthy, NF1 and NF2 fibroblasts

Rufeng Ma[1,2], Xiangyu Gong[1,2], Kristen Mills[1,2]

1 Department of Mechanical, Aerospace, and Nuclear Engineering/Rensselaer Polytechnic Institute, Troy, NY 12180
2 Center for Biotechnology and Interdisciplinary Studies, Rensselaer Polytechnic Institute, Troy, NY 12180

contact: mar6@rpi.edu

Cells sense the physical properties of their extracellular environment and translate them into biochemical signals. Neurofibromatosis type 1 (NF1) and Neurofibromatosis type 2 (NF2) are two tumor-associated genetic disorders in which the proteins encoded are involved in the cell mechanosensing or motility pathways. The neoplastic origin of neurofibromas, benign tumors associated with the disease, are believed to be NF1- deficient (NF1-/-) Schwann cells, and haploinsufficient (NF1+/-) stromal cells, such as fibroblasts. Little work has been invested to study the mechanobiology of these cells. Here we studied the mechanosensing ability and motility of healthy, NF1+/-, and NF2+/- fibroblasts on 2D microgroove-patterned substrates and in 3D collagen matrix.

Silicon wafers were produced by photolithography and used as molds for transferring the topographical patterns into biocompatible polydimethylsiloxane (PDMS) substrates. The patterns consist of several rectangles with parallel grooves of different groove widths. The patterned PDMS substrates were coated with collagen prior to cell seeding.

Here we present the alignment, migration, and contractile behavior of fibroblasts from healthy, NF1, and NF2 patients. We report, for the first time, evidence of significantly reduced contact guidance of NF2 fibroblasts as compared to both healthy and NF1 fibroblasts when cultured on submicron topographies. Correspondingly, we observed abnormal shape and a poorly organized actin cytoskeleton in NF2 fibroblasts. Traction force experiments revealed that NF2 fibroblasts also produce significantly lower traction force (10-25 nN) than healthy or NF1 fibroblasts (30-40 nN). Characterization of the FA development by the cells on the patterned substrates indicated that topography may regulate FA size [1].

Conclusion: Compared to healthy and NF1 fibroblasts, NF2 fibroblasts displayed reduced contact alignment ability on 2D micropatterns in addition to lowered traction force-generating capability. These results will be important in determining the biomechanics of tumor development in NF1 and NF2.

Reference: R. Ma, X. Gong, J. Kulwatno, O. Fedoniuk, R. Kemkemer, D. Kaufmann, and K.L. Mills (2018). Linking the Mechanosensing Ability of Fibroblast Cells to Their Force- Generating Capabilities. Manuscript under review

PP.25 LAUREN BRADY
12:45 – 1:45

NSF Hurricane Harvey: Ultrasensitive photodetector development for high throughput bacteria detection in floodwater

Lauren Brady[1], Dali Shao[1], Debjit Ghoshal[2], Shayla Sawyer[1], Valencia Koomson[3]

1 Department of Electrical and Computer Systems Engineering, Rensselaer Polytechnic Institute
2 Department of Chemical and Biological Engineering, Rensselaer Polytechnic Institute
3 Department of Electrical and Computer Engineering, Tufts University

contact: bradyl@rpi.edu

Flooding after major hurricanes such as Hurricane Harvey can have long term consequences on water quality and human health. Pathogenic bacteria found in floodwaters present unique dangers as significant quantities of these pathogens can remain active for several months after a catastrophe happens, posing a hidden threat to those affected by natural disasters. By improving the synergistic properties of nanocomposites to create an ultrasensitive ultraviolet (UV) detector, the goal is to identify and quantify bacteria in floodwaters in real time. Intrinsic fluorescence serves as our detection mechanism for optical analysis, as these microbes will fluoresce when excited in the UV range. Our previous ultrasensitive UV light detector was created using a highly conductive graphene channel and a ZnO quantum dot (QD) layer, with a 10-decyltrichlorosilane organic self-assembled monolayer (SAM) interface, to reduce the impacts of charged impurity scattering and other scattering mechanisms on the carrier mobility. Experimental results from our device show a high photoresponsivity of 10^8 A/W, an increase in the carrier mobility to 10,800 $cm^2V^{-1}s^{-1}$, and a gain of 3 $x10^9$ in the UV region. To improve device performance, alternatives to the SAM layer are explored to decrease the dark current output, and QDs with different absorption wavelengths are explored to improve photoresponsivity. The goal is to integrate these devices into a frequency domain spectrometer circuit architecture that will allow for the creation of a sensor network that can be deployed real time. The effects of graphene and QD layers on dark current, photoresponsivity, and time response are also investigated with the extension of these findings being utilized to improve the simulation of photodetectors with these structures in NEMO5.

PP.26 YOUNG HWA KIM
12:45 – 1:45

Nanofabrication of Active and Passive Silicon Optical Modulator

Young Hwa Kim[1], Alexander Chen[2], Lingjun Jiang[1], Stephen Anderson[1], Zhaoran Huang[1]

1 Electrical Engineering and Computer and System Engineering, Rensselaer Polytechnic Institute, Troy NY, 12180
2 Physics, Applied Physics, and Astronomy, Rensselaer Polytechnic Institute, Troy NY, 12180

contact: kimy15@rpi.edu

Recent development of the silicon photonics technology has enabled numerous compact and low-cost on-chip optical systems with various functionalities. Based on the configurations of the physical structure and the electrical properties of silicon photonic devices, their applications categorize into slow light waveguides and optical interconnect waveguide. Passive silicon photonic device intended for slow light application comprises mode-transition grating structures that achieve impedance match at the grating/waveguide interface by inserting a short, tapered grating segment that has a group index smaller than the main section of the slow-light Bragg grating waveguide. Active silicon photonic device on the other hand, is intended for high speed optical transmission and it incorporates depletion mode interleaving PN junction in order to maximize the free carrier plasma effect to achieve intensity modulation. The key aspect is to maximize the depletion layer in the path of the light in order to minimize the optical loss with high speed. In this poster, we present the key nanofabrication works to fabricate the waveguide of electrically passive and active devices for the slow light devices and the optical interconnect applications respectively.

Acknowledgements: ARL, AFRL, and BNL

PP.27 JENNIFER HOWELL-CLARK
12:45 – 1:45

Advanced Gate Oxide Processes for Robust and High-Performance 4H-SiC MOSFETs

Jennifer Howell-Clark[1,2], Xiang Zhou[2], Collin Hitchcock[2], Ishwara Bhat[2] and T. Paul Chow[2]

1 Physics, Applied Physics, and Astronomy, Rensselaer Polytechnic Institute, Troy NY 12180

2 Electrical, Computer, and Systems Engineering Department, Rensselaer Polytechnic Institute, Troy, NY 12180

contact: howelj2@rpi.edu

Silicon Carbide (SiC) power devices have the potential to deliver greatly increased performance versus traditional silicon devices, enabling power electronic systems which are lighter, smaller, more efficient, and more tolerant of high temperatures. Many of the most common device structures in silicon technology, such as metal-oxide-semiconductor field effect transistors (MOSFETs), can also be fabricated in silicon carbide, allowing for SiC devices to serve as drop-in upgrades to silicon power devices – meaning that existing circuits and power systems can be improved by substituting SiC devices for silicon counterparts, without the need for major modifications of the circuit design.

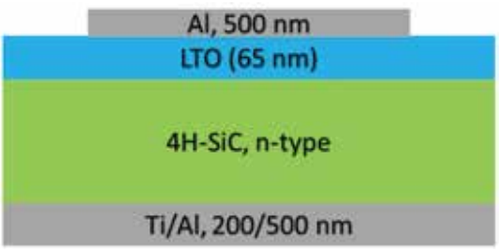

Figure 1. Cross-section of MOS Capacitor structure used to study MOS interface properties

Like silicon, SiC can form a thermally grown silicon dioxide (SiO_2) layer by exposing a wafer surface to an oxidizing ambient at high temperatures. However, unlike silicon, the interface formed between SiC and SiO_2 grown in this way is poor, with many defects that trap or scatter electrons, leading to poor electron mobilities in MOS channels and device performance that falls significantly short of the material's potential. Replacing thermally grown oxide with a deposited SiO_2 layer, followed by subsequent annealing in nitric oxide (NO) ambient, has been shown to greatly improve the field-effect mobility in SiC MOS channels by introducing nitrogen to the interface, passivating many of the defects that trap carriers. However, MOS gates fabricated in this way have an unacceptably high degree of threshold instability, with the threshold voltage drifting by 200 mV or more under high-temperature stressing. We report on several more sophisticated processes which aim to achieve both high electron mobilities and stable threshold voltages via annealing in NO, N_2, N_2O, and other ambients, and using quantitative capacitance-voltage (CV) and conductance-based measurements to form a complete physical picture of the SiC/SiO_2 interface as a function of process conditions.

PP.28 ZHIZHONG CHEN
12:45 – 1:45

Remote Phononic Effects in Epitaxial Ruddlesden-Popper Halide Perovskites

Zhizhong Chen[1], Yiping Wang[1], Xin Sun[2], Yu Xiang[2], Yang Hu[1, 2], Jie Jiang[1], Gwo-Ching Wang[2], Toh-Ming Lu[2], Esther A. Wertz[2], Jian Shi[1]

1 Department of Materials Science and Engineering, Rensselaer Polytechnic Institute, Troy, NY 12180

2 Department of Physics, Rensselaer Polytechnic Institute,, Troy, NY 12180

contact: chenz15@rpi.edu

Despite their weak nature, van der Waals interactions have been shown to be effective for controlling the optoelectronic and vibrational properties of layered materials like graphene and transition metal dichalcogenides. However, how such van der Waals effects exist in Ruddlesden- Popper layered halide perovskites remains unclear. In this work, we reveal the role of the interlayer van der Waals force in Ruddlesden-Popper phase perovskite in regulating its phase transition kinetics and carrier dynamics, based on the high quality epitaxial single crystalline $(C_4H_9NH_3)2PbI_4$ flakes with controlled dimensions. Based on spectroscopy studies, we show that both the substrate-perovskite epitaxial interaction and the interlayer van der Waals interaction play a significant role in suppressing the structural phase transition. Electron-phonon coupling strength is revealed to be highly thickness-dependent suggesting the ineffectiveness of phonon confinement of the natural quantum wells in two-dimensional halide perovskites. It is demonstrated that with reducing flake thickness from ~100 nm to ~20 nm, electron-phonon coupling strength decreases by around 30%. These discoveries show that the conventional understanding that Ruddlesden- Popper halide perovskite is equivalent to a multiple quantum well structure has to be substantially amended due to the existence of the significant nonlocal phononic effects in the layered crystal in which intralayer interaction is not drastically different from the interlayer force.

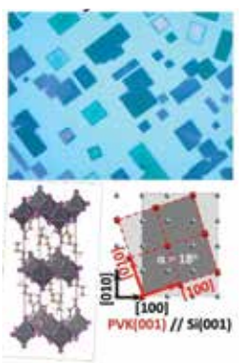

Acknowledgements: This project was supported by US National Science Foundation under award number 1635520 and Office of Naval Research under award number N000141812408

PP.29 RAJENDRA DAHAL
12:45 – 1:45

Hexagonal Boron Nitride for Deep Ultraviolet Photonic

Rajendra Dahal[1], Kawser Ahmed[1], James Jian-Qiang Lu[1], Yaron Danon[2], and Ishwara B. Bhat[1]

1 Department of Electrical and Computer Systems Engineering, Rensselaer Polytechnic Institute, Troy, NY, 12180
2 Department of Mechanical, Aerospace, and Nuclear Engineering, Rensselaer Polytechnic Institute, Troy, NY, 12180

contact: dahalr@rpi.edu

Hexagonal boron nitride (hBN) is a layered material with unique features of ultra-wide bandgap (~6 eV), high in-plane thermal conductivity, low density, high temperature resistance under extreme conditions, low dielectric constant, chemical inertness, and negative electron affinity. These properties make hBN an ideal candidate for deep-UV light emitters, detectors, and electron emitters in field emission. Furthermore, as structural analogs of graphene, two- dimensional hBN can serve as an excellent gate dielectric as well as substrate for graphene devices. The atomically flat hBN layer provides a smooth and flat interface without dangling bonds, which is a highly desired characteristic for high-carrier mobility devices. hBN growth was carried out on (100) sapphire and (111) Si substrates at a temperature of 1300 to 1350 C using a cold wall chemical vapor deposition system. The hBN phase of the deposited films was identified by the characteristic Raman peak at 1370 cm^{-1} with a full width at half maximum of 25 cm^{-1}, corresponding to the in-plane stretch of B and N atoms. Chemical bonding states and composition of the hBN films were analyzed by X-ray photoelectron spectroscopy; the extracted B/N ratio was 1.03:1, which is 1:1 within the experimental error. Metal-hBN-metal deep UV detectors were fabricated on both free standing hBN and hBN grown on Si substrate. These hBN films demonstrate a strong deep UV response. Further, the in-plane and out-of-plane mobility– lifetime products of electrons and holes in free-standing hexagonal boron nitride (hBN) films are extracted from current–voltage characteristics of metal–hBN–metal structures measured under external excitations. The mobility–lifetime product is a few orders of magnitude higher along the plane than along the out of plane in hBN films.

PP.30 NATE KIMMITT
12:45 – 1:45

Investigating Light-Matter Interactions Through the Coupling of Single Emitters to Bowtie Nanoantennas

Nate Kimmitt[1], Zach Hallenbeck[1], Esther Wertz[1]

1 Physics, Applied Physics, and Astronomy, Rensselaer Polytechnic Institute, Troy NY, 12180

contact: kimmin@rpi.edu

Metallic nanopoarticles, which confine light into very small volumes and greatly enhance fields, have many exceptional and tunable optical properties. Nanodimers known as bowtie nanoantennas are known to have strong field enhancements and confinement to the gap between the triangles. However, due to intrinsic ohmic losses, obtaining strong coupling between an emitter and the cavity remains an issue.

In this study, to elucidate the effects of the nanometric positioning of the emitter, we employ super-resolution single-molecule fluorescence techniques to study the effects of detuning, incident polarization, substrate orientation, nanometer gap size, and adhesion layer have on the fluorescence properties of the dye, as well as the trapping dynamics of the system.

The arrays were fabricated using electron beam lithography and aided by BEAMER, which takes into account electron scattering effects, field aberrations, and stitching to optimize the pattern data, obtaining sharper feature sizes. Nanobowties with as small as 70nm side length and sub-10nm gaps were fabricated.

A clear set of optimal parameters has been found, aided by finite element simulations in COMSOL, hinting towards obtaining the maximal coupling for single emitters in this geometry.

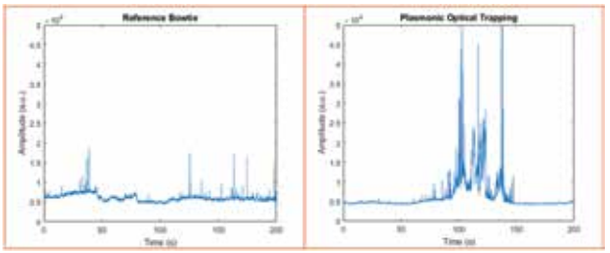

PP.31 SHADY GOMAA

12:45 – 1:45

Identifying the Chloride Content Threshold for Rebar Corrosion in Concrete

Shady Gomaa[1], David Duquette[2], Mohammed Alnaggar[1]

1 Civil and Environmental Engineering, Rensselaer Polytechnic Institute, Troy, 12180,
2 Material Science and Engineering, Rensselaer Polytechnic Institute, Troy, 12180

contact: alnagm2@rpi.edu

Chloride-induced corrosion of steel is considered to be one of the major causes of degradation of reinforced concrete structures. Once the passive layer around the rebar is compromised due to ingress of chloride ions through concrete, anodic and cathodic sites start to form on the steel surface that create micro-corrosion cells soon to grow into macro ones.

In this study, the corrosion sensitivity of polished reinforcing steel rebars in a synthetic concrete pore solution environment with varying chloride ion concentrations has been performed by the Anodic Polarization Sweep method. The use of synthetic pore solutions eliminates the variability encountered from the diffusion through the porous cracked concrete matrix yet mimics the chemical conditions near to the rebar surface. The chloride content was varied from 0 to 0.6M with 0.1M step increments. For each concentration, and three replica were tested to reduce the experimental scatter. 500mL synthetic concrete pore solution was prepared using the desired chloride content and stirred for five minutes. The solution's Potential of Hydrogen (pH) was measured for every specimen and its range was 12.9-13.3. The corrosion cell was set up in two stages. In the first stage, the cell is left for 10 mins in open circuit Potential (OCP) to rest, next, it is polarized cathodically at 1.0 volt for another 10 mins to remove the existing passive film, then it is left in open circuit for 40 mins to rest again. In the second stage, anodic sweep from OCP to 1.5 Volts above reference is performed with a scan rate of 0.03125 mV/s. All specimens were tested under aerated condition using atmospheric air. The results showed that the presence of chloride ions reduces the ability of steel to resist depassivation. Corrosion initiation potential above OPC is increased with increasing the solution's pH and decreasing the chloride content. To investigate the effects of limited oxygen ingress during early uncracked stages of corrosion in real structures as well as accelerated corrosion tests performed in the lab, additional specimens were tested in a de-aerated environment with argon gas. Results have shown a clear increase in the potential with de-aeration which indicates increased corrosion resistance.

Acknowledgements: Michael Kubista

PP.32 TATHAGATA BHADURI

12:45 – 1:45

Understanding Load Transfer Mechanisms During Failure of Ultra High-Performance Concrete (UHPC) Beams

Tathagata Bhaduri[1], Mohammed Alnaggar[1]

1 Department of Civil & Environmental Engineering, Rensselaer Polytechnic Institute, Troy, 12180

contact: bhadut@rpi.edu

Ultra High Performance Concrete (UHPC) belongs to a specific class of cementitious composites which attains high compressive strength (~150 MPa) and is capable of exhibiting high ductility when mixed with a proper fraction of discrete fibers. Due to heterogeneity at the microstructural level as well as the quasi-brittle nature of its cementitious matrix, macro scale continuum-based models can not replicate complex micromechanics including fiber bridging, crack localization, coalesense and progression. In contrast, mesoscale discrete models like the Lattice Discrete Particle Modelling (LDPM) can represent the material heterogeneity by a realistic representation of its main constiuents at the meso-scale (coarse aggregate scale). LDPM represents the matrix through an assemblage of interacting spherical particles that are randomly sampled and placed based on the actual grain size distribution of the UHPC matrix. The interparticle interfaces (called facets) are the locations over which, vectorial stress-strain measures are defined. LDPM constitutive laws differentiate between cohesive fracturing during tension, strain hardening during compression accounting for pore collapse during material compaction and frictional behavior during shear. To represent fibers, an extended version of LDPM called LDPM-F randomly introduces the fibers into the volume and their contributions are added at their intersections with the discrete interfaces (facets) between the aggregate pieces. In the current study, LDPM mesoscale variables are identified with companion tests like three-point notched bending, split tension and uniaxial compression test. Moreover, the fiber contribution is calibrated based on microscale phenomena like debonding slip, micro-spalling, snubbing etc. A comprehensive experimental program is designed which includes two UHPC beams with single and double rebars. To uncover the effect of fiber on shear behavior and failure modes, fiber content is varied from 0 to 2%. Excellent agreement is observed in predicting shear behavior and failure modes of UHPC beams. By using this comprehensive modeling framework, the different contirbutions of various load transfer mechanisms (fibers bridging, aggregate interlocking, ...) during loading up to failure were uniquely identified.